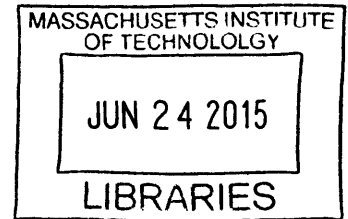It's Getting Hot in Here: Temperature Gradients in Lithium-Ion Battery
Packs

by

Benjamin Niewood

Submitted to the
Department of Mechanical Engineering
in Partial Fulfillment of the Requirements for the Degree of

Bachelor of Science in Mechanical Engineering

at the

Massachusetts Institute of Technology

June 2015

Signature of Author: _____ Signature redacted _____

Department of Mechanical Engineering
May 8, 2015

Signature redacted

Certified by: _____

Sanjay E. Sarma
Professor of Mechanical Engineering
Thesis Supervisor

Signature redacted

Accepted by: _____

Anette Hosoi
Professor of Mechanical Engineering
Undergraduate Officer

Temperature Gradients and Cooling in Lithium-Ion Battery Packs

by

Benjamin Niewood

Submitted to the Department of Mechanical Engineering
on May 14, 2015 in Partial Fulfillment of the
Requirements for the Degree of

Bachelor of Science in Mechanical Engineering

ABSTRACT

A 5 channel, 40A battery cycler was constructed for the purpose of carrying out thermal studies on Lithium-ion battery packs. Boston Power Swing Key 442 battery blocks were tested to determine the magnitude of the temperature gradient over the pack. The battery blocks were stacked vertically, similar to how they might be situated on an electric vehicle. They were cycled, discharged then charged, at a current of 40A in stacks of one, two, three and four, with and without unidirectional air-cooling from the top of the pack. The resulting temperature data was analyzed to see if a temperature gradient over the pack was present. A correlation was found between placement in the pack and cell temperature; the lower down in the pack a cell was, and thus the further from the air flow, the warmer the pack became during operation. For the four battery test, a maximum temperature difference of 2.9°C was observed between the hottest and coldest cells.

Thesis Supervisor: Sanjay E. Sarma
Tile: Professor of Mechanical Engineering

Acknowledgements

There are so many people who helped me get to this point in my life, to finishing both my thesis project and MIT, that I would like to thank here. First, I would like to thank my advisor, Professor Sanjay Sarma for allowing me to work in his lab and for helping me throughout the project. Without his support I never could have accomplished what I did over my last years as an undergraduate. Thank you to Boston Power for sponsoring my research and for giving me the battery cells to work with. Thank you to Stephen Ho and Isaac Ehrenberg for giving me support and ideas throughout the project and for always being up for kosher lunch.

I would like to give a huge thank you to Josh Siegel for giving me the opportunity to work on this project in the first place, for always being there for class or project help or to have fun, and for helping me immensely through my mechanical engineering experience at MIT. I took more advice and direction from you over the past four years than you probably know, and without it my time here would not have been nearly as successful as it was.

I would also like to give an enormous thank to my research partner, Dylan Erb. Your constant support, teaching and understanding made this project not only possible but also fun. While I know that I may not have always been on top of my assignments, and while I almost never stuck to the schedule we set up, you always understood when I had other obligations and were willing to make it work. I learned so much from you over the past two years and am so grateful that I had the opportunity to work with you.

Last but not least, I would like to thank my parents for everything they have done for me in life and my fiancé Aliza for always being right beside me and for understanding, or at least tolerating, the long hours in class, lab, the shop and meetings that have been necessary to get me through my classes and projects.

1 Background

1.1 Automobile History

The first automobile is said to have been a steam-powered vehicle invented by Nicolas-Joseph Cugnot in 1768. Over a century later, in the 1890s, automobile production increased significantly and three main propulsion technologies competed for the United States market: electric, steam and gasoline. [1] In 1899 there were more steam and electric than gasoline cars on the road in the US. All three technologies had advantages and disadvantages. Steam powered automobiles needed to warm up for a significant time before they could be used and they required huge amounts of water. Electric cars could not climb steep hills, had short ranges and low top speeds [1]. Gasoline cars were noisy and difficult to start and also had the same problems as electric vehicles. Early hybrid vehicles had many of the same problems as electric and gas vehicles and were also less powerful and more expensive. It was not until the 1920s that cars powered by fossil fuels alone emerged as the clear winner.

In the first two decades of the 20th century gasoline carmakers, and especially Henry Ford, solved many of the issues related to gasoline cars; they reduced the noise, vibration and odor of the cars' engines enough so that consumers were willing to buy them. In the 1920s the self-starting gasoline engine was invented and this, coupled with gasoline's high energy density and low price, led to the internal combustion engine's (ICE's) victory [2]. Since then, ICE cars have dominated the market.

1.2 Problems with Gasoline Powered Vehicles

While gasoline powered car efficiency has increased significantly over the years, they still have significant problems that have not been solved. While their noise was reduced enough for consumers in the early 1900s, today with the high number of cars on the road the noise pollution in urban areas is significant. In addition gasoline powered cars contribute hugely to pollution. It is estimated that anywhere from 50-90% of smog and ozone pollution in urban areas, and around 75% of carbon monoxide emissions and greenhouse gases, comes from cars [3]. Even though cars have higher and higher miles per gallon ratings, the increasing number of cars on the road every day leads to ever rising pollution numbers. Today gasoline is also relatively expensive, and, while prices fluctuate constantly, in general the price per gallon of gas is constantly rising. Furthermore, while estimates on when the world will run out of oil vary greatly, most agree that within 100 years the world will reach peak oil production and within 200 we will run out of the world's supply of naturally occurring oil. Once this happens gasoline powered cars will become economically infeasible unless biofuels become much cheaper. While this may not be an immediate problem, clearly the world needs to start revisiting or inventing alternative energy vehicles to deal with these problems.

1.3 Alternate Fossil Fuel Vehicles

In the 1970s the price of gasoline rose sharply during the Arab oil embargo, leading to renewed interest in alternative energy vehicles. While steam powered cars have all but vanished, a number of other alternative energy cars are in production today. Natural gas powered cars are cleaner burning than their gasoline counterparts, and are in fairly wide use in much of the world (about 18 million were on the road in the world in 2013 Still, they also contribute to pollution and rely on a resource that is also running out. Hydrogen gas and hydrogen fuel cell powered cars have come and gone over the years, and recently have seen somewhat of a resurgence with cars like the 2015 Toyota Mirai, one of the first hydrogen powered cars to be sold commercially. Still, these are not by any means in wide use and their rocky history does not indicate that they will make a true resurgence anytime soon.

1.4 Electric Cars and Hybrids

1.4.1 Hybrid Cars

Two of the most promising technologies that have come back in recent years are the electric and hybrid vehicle. In 1997 the Toyota Prius, the first new hybrid electric vehicle, was introduced in Japan and in 1999 the Honda Insight became the first new hybrid to make its way to the US. These cars helped reduce the gasoline consumption of a traditional automobile in a number of ways. They are particularly useful in urban areas where there is significant stop and go traffic since the engine can shut off during idling and because the frequent braking can be used to charge the battery, recovering much of the energy usually lost to heat. This regained energy from regenerative braking is stored in the car's batteries and can then be reused to power the car during peak use times, increasing its mileage per gallon of gas. Still, these cars need gasoline to work and also still release greenhouse gases and contribute to smog and ozone depletion.

1.4.2 Electric Cars

Another available option that is now gaining popularity is the fully electric car. In 2014 there were around 700,000 fully electric cars on the road, compared to around 18 million hybrid cars and over a billion gasoline powered cars [21-23]. In 2008 the Tesla Roadster was introduced and became one of the first modern fully electric cars with over a 200-mile range. Sales of fully electric cars have since been on the rise, especially since 2010 with the introduction of the Nissan Leaf, one of the first new mass production fully electric vehicles. Since then carmakers all over the world, including BMW, Chevy, Fiat, Ford, Kia, Mercedes, Mitsubishi, and more have ramped up design and production of fully electric vehicles.

1.4.3 Problems with Electric Cars

Significant problems still exist that keep the world from fully adopting electric vehicles. While electric cars today can be just as powerful, if not more so, than gasoline powered cars, much of the world still sees them as unappealing as golf carts [5]. There is also a huge lack of infrastructure since there are not enough charging stations to support many more sales. This lack of infrastructure, coupled with the perception that the vehicles do not have a large enough range on a single charge, is a significant barrier for many consumers. While electric cars are getting cheaper, they are often still more expensive than ICE cars. Finally, there is much debate over whether they are actually better for the environment. Some believe that the environmental cost of mining the elements needed to produce the batteries, combined with the energy cost of charging the vehicles, is enough to make them as bad as or even worse for the environment than fossil fuel powered vehicles. This is mainly because charging the vehicles requires energy produced from power plants that often burn coal to produce said energy. The amount of greenhouse gases produced from charging an electric vehicle for a trip can then be the same or larger than the amount produced by an electric car travelling an equivalent distance. If the world is able to replace coal power plants, however, with sustainable energy options, like nuclear, wind and hydroelectric, then electric vehicles present a significant environmental advantage over fossil fuel powered cars [6-8].

2 Energy Storage Fundamentals

2.1 Different Types of Batteries Available

While batteries were not a viable power source for cars initially, significant strides in battery technology have been made in the last few decades. This development has especially exploded in the latter part of the 20th century due to the need for batteries in commercial electronics.

Initial cars in the early 1900s used lead acid batteries that had a specific energy of around 18 Wh/kg . This number has since risen to around 30-40 Wh/kg. That is still nowhere near gasoline's 6,500 Wh/kg, assuming a typical Otto cycle, and is not viable as an option for electric road cars [9-10].

Nickel-cadmium batteries were developed in the 1980s and now have a specific energy of around 50 Wh/kg. They are fast charging, have good specific power and a good cycle life, however they are expensive and there are environmental concerns with using cadmium in the batteries [9-10].

Nickel-metal hydride batteries have a specific energy of around 60-70 Wh/kg. The Toyota Prius currently uses nickel-metal hydride batteries mainly because of their production cost and their relatively high specific power. NiMH batteries do, however, have a significant memory effect. This means that when a NiMH battery is recharged before it is fully depleted it will suffer a small capacity loss. Over time these losses build up and cause the pack to die more quickly than it would if it were discharged fully before being recharged [9-10].

Currently the most promising battery for electric vehicles is the lithium-ion battery. They have a specific energy range of 100-265 Wh/kg with the potential to reach nearly 2000 Wh/kg. This makes a lithium ion battery pack with a similar energy density much lighter and smaller than its NiMH counterpart [9-10]. Li-ion cells also do not suffer from the same memory effect that NiMH battery packs do. Li-ion batteries are already used in many electric cars today, like the Tesla and the Nissan Leaf. Toyota will also soon be replacing the Prius's NiMH pack with a Li-ion one due to its higher energy density and lack of memory effect.

Figure 1: The nickel-metal hydride battery pack from a Toyota Prius. The battery has a nominal capacity of 4.4 kWh and weighs around 110 pounds (source: forbes.com)
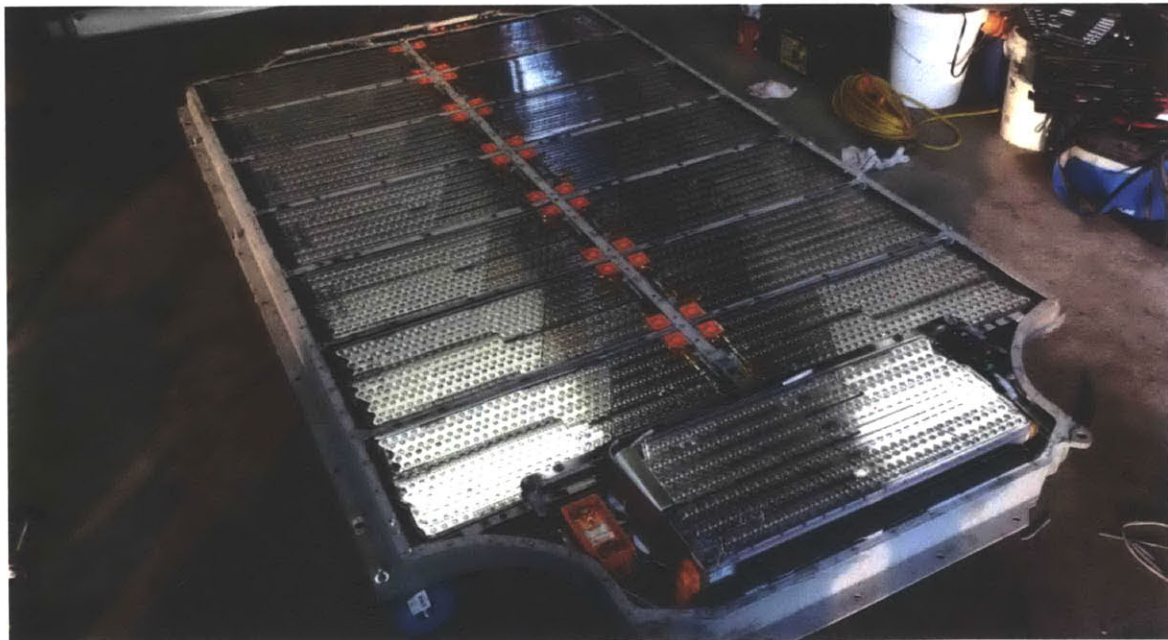
Figure 2: The battery pack from a Tesla Model S. This pack has a capacity of 85kWh and weighs 1,200 lbs. (source: insideevs.com)

8

Figure 3 shows the Ragone chart for various types of batteries. This chart is used to compare the performance of different types of energy-storage devices. Here the specific power in W/kg is plotted against the specific energy in Wh/kg. Using this chart it is easy to compare the different types of batteries for various applications. In hybrid vehicles, high specific power is generally more important and in fully electric vehicles high specific energy is important [9]. As the cart shows, Li-ion batteries can be optimized for a wide range of power to energy ratios, making them suitable for a large number of tasks.
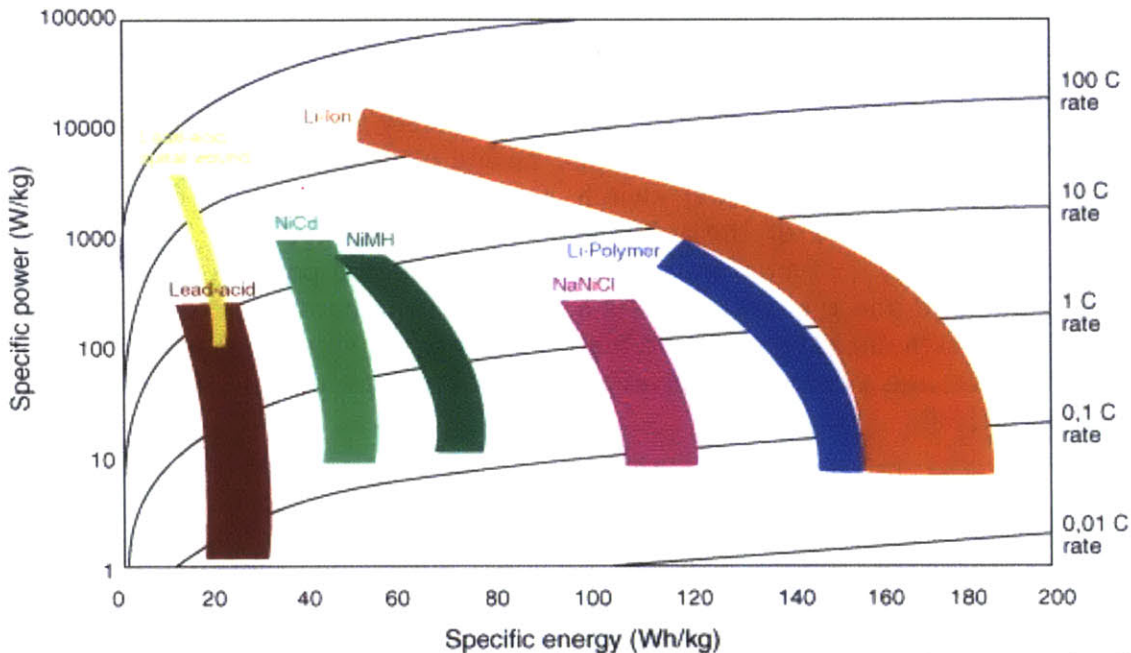
Figure 3: The Ragone Chart. Here specific power is plotted against specific energy. The chart can be used to find the proper battery for use in various applications based on its comparative performance in energy density and power density [9]

2.2 Lithium-ion batteries

2.2.1 History

Lithium was first proposed as an electrode for batteries in the 1970s. In 1991 the first commercial Lithium-ion battery was released and since then significant improvements have been made in their energy density and efficiency. Lithium-ion batteries are the battery of choice for many portable consumer electronics because of their easy re-chargeability, high energy density and ability to hold a charge for relatively long periods of time when not in use. As mentioned above, today they are also popular in electric vehicles.

2.2.2 Operation

9

Batteries store energy through reversible, exothermic, electrochemical reactions. A voltage is applied between the positive and negative electrode, forcing the ions in the electrolyte to move between them. When charging, the voltage is applied so the lithium-ions move to the negative electrode. When discharging, the ions migrate back to the positive electrode, producing a voltage and allowing current to flow through an external circuit.

2.2.3 Construction

Lithium-ion batteries are made of five main components, the anode, or positive electrode, the cathode, or negative electrode, the separator, for preventing the electrodes from shorting out, the electrolyte, to provide the moveable ions, and the can, to enclose the cell. There are also a number of safety mechanisms in most li-ion cells, such as safety vents, for allowing the escape of pressurized gas, or the PTC (positive temperature coefficient) switch, for shutting the battery off before it overheats. The structure of the li-ion cell is shown in Figure 4. The negative electrode is typically a carbon material, often graphite, the positive electrode is a lithium compound and the electrolyte is a lithium salt in an organic solvent. Both the anode and cathode have an active material, which provides a lattice for storing the lithium-ions, and a current collector that gives a path for current to move in and out of the cell [10].
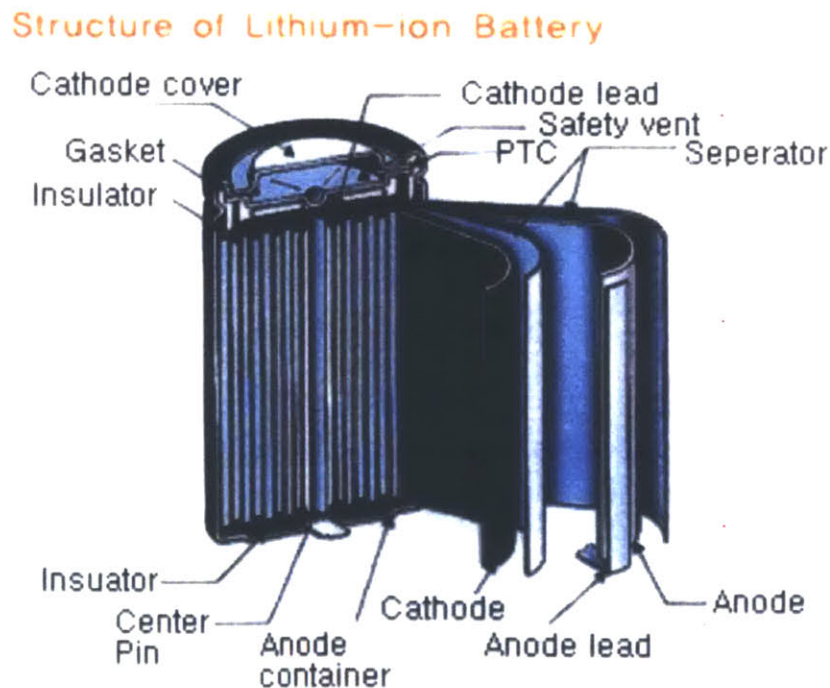

Figure 4: The structure of a cylindrical lithium-ion cell with components labeled (source: gm-volt.com)

10

Figure 5 shows how a li-ion cell operates when charging and discharging. In both cases, the ions available in the electrolyte move against the direction of the current, through the separator and into the opposite electrode. When discharging the ions move towards the cathode, producing a voltage and powering whatever the battery is connected to.
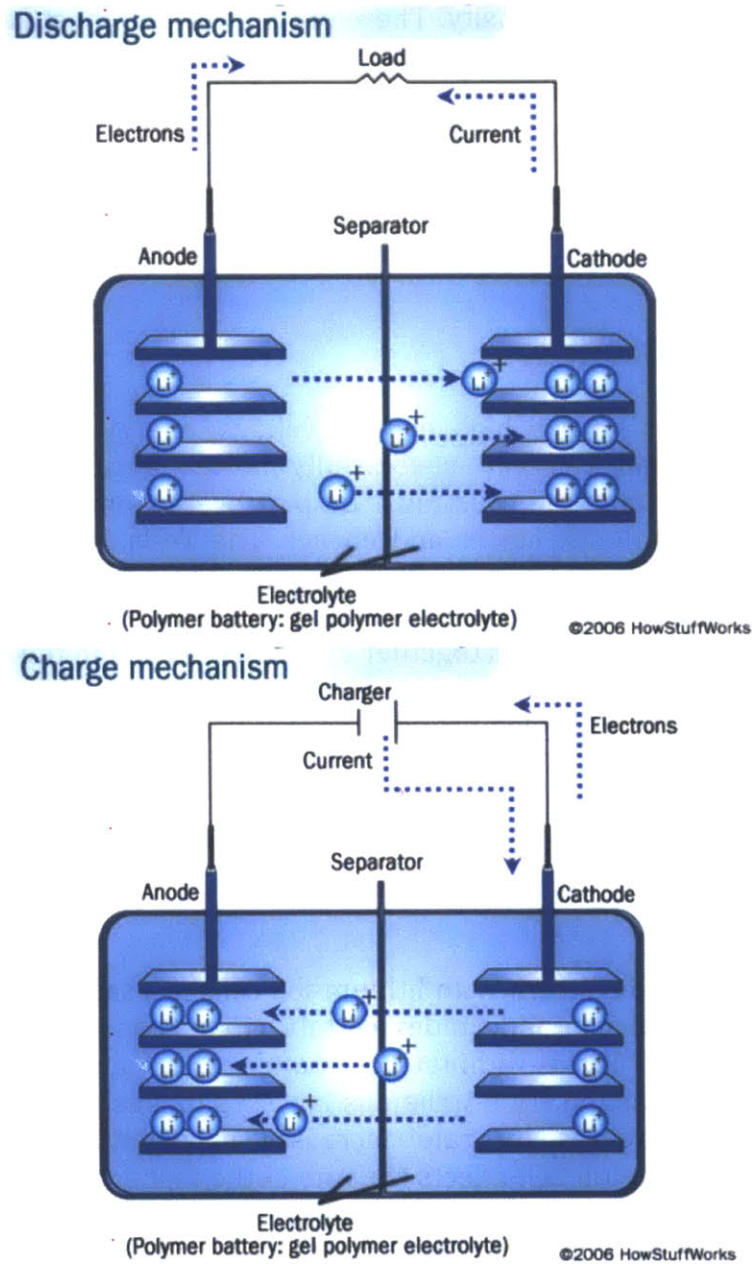

Figure 5: What happens inside a battery when it charges and discharges. The lithium ions move between the anode and the cathode, through the separator. During discharge the movement towards the cathode produces a voltage (source: howstuffworks.com)

2.2.4 Design Variability

11

Since all of these materials must fit in a fixed space tradeoffs must be made between power and energy density. To increase power capacity the volume of the current collector must go up, which, assuming the size of the cell and the remaining components remain constant, leads to a corresponding decrease in the size of the active material. The active material stores the batteries energy so less active material means lower energy density. Therefore a given cell must sacrifice energy density to get the power density required for the application. Furthermore, depending on the specific material choices, the batteries can be optimized for voltage, energy density, power density, life and safety. All of these design considerations must be taken into account when making a lithium-ion cell and it also means the cells can be optimized for a variety of applications.

3 Motivation

3.1 Importance of Pack Design

Single lithium-ion cells have a high enough voltage, energy density and power capacity that one small cell can successfully power a cellphone. For larger applications, however, multiple cells must be put together into a battery pack to achieve the required voltage, power and energy. The Tesla Model S uses around 7000 small, laptop-sized cells to power its cars while other electric vehicles, like the Nissan Leaf, use fewer, larger cells. Unfortunately designing a car's battery pack is not as simple as wiring all the cells together and shoving them in the car. One of the many considerations that goes into designing a battery pack and the associated systems is keeping the cells cooled properly so that they operate within the correct temperature range.

3.2 Thermal Management

3.2.1 Safety Concerns

One temperature related concern with lithium-ion cells is a safety one. Lithium-ion cells heat up in normal use and, under certain circumstances, can rupture and explode. As described above, lithium ion batteries produce energy from an exothermic chemical reaction. The Arrhenius law says that as the temperature of a chemical reaction increases its rate increases exponentially. Therefore the temperature of a lithium-ion cell affects the rate of the reaction going on inside the cell. Normally this is not a problem since the cells can be kept at a low enough temperature to ensure that the reaction is not affected significantly. If the temperature of a lithium-ion cell gets to around 60-80°C (depending on the chemical composition of the cell) however then the cell can enter a state called thermal runaway. Thermal runaway here is a term used to describe an uncontrolled positive temperature feedback loop of the chemical reaction in the cell [12].

For most types of lithium-ion cells, thermal runaway happens in the following manner. First the cell heats up because of overcharging, high external temperature, improper temperature dissipation, short circuit or excessive currents. Once the cell reaches around 80°C the solid-electrolyte interface (SEI), a thin, passivating layer of carbonated compounds on the surface of the anode, breaks down. The electrolyte can then react with the anode exothermically and as it does the cell heats up further. As the cell continues to heat up the organic solvents in the electrolyte break down, releasing ethane, methane and other, flammable, hydrocarbon gases. This breakdown typically starts at around 110°C but can start at temperatures as low as 70°C for some electrolytes [11-13].

As these gases build up, so does the pressure inside the cell, but although the temperature inside the cell is higher than these gases' flashpoints the cell does not yet ignite since no free oxygen is present to sustain a fire. Typically lithium ion cells have safety vents that allow these gases to be vented into the air so that the pressure in the cell does not go so high as to rupture the cell. Once these gases reach the air they can catch fire and burn, but this is safer than waiting for them to cause the cell to explode. Still, these safety vents may not work properly or can become obstructed or overwhelmed and the cell can continue to heat up while more gas is created. At around 135°C the separator melts and the electrodes short circuit. As the cell's temperature rises the metal oxide cathode breaks down releasing free oxygen into the gas-filled cell and allowing the gases to start a sustained fire. The cathode breakdown happens at various temperatures for different battery chemistries but for some typical batteries it is around 200°C. This breakdown is also a highly exothermic reaction and causes the temperature in the cell to rise even further [11-13].

1. Heating starts.

2. Protective layer breaks down.

3. Electrolyte breaks down into flammable gases.

4. Separator melts, possibly causing a short circuit.

5. Cathode breaks down, generating oxygen.

ANODE (CARBON)

PROTECTIVE LAYER

ELECTROLYTE
(lithium salt in organic solvent)

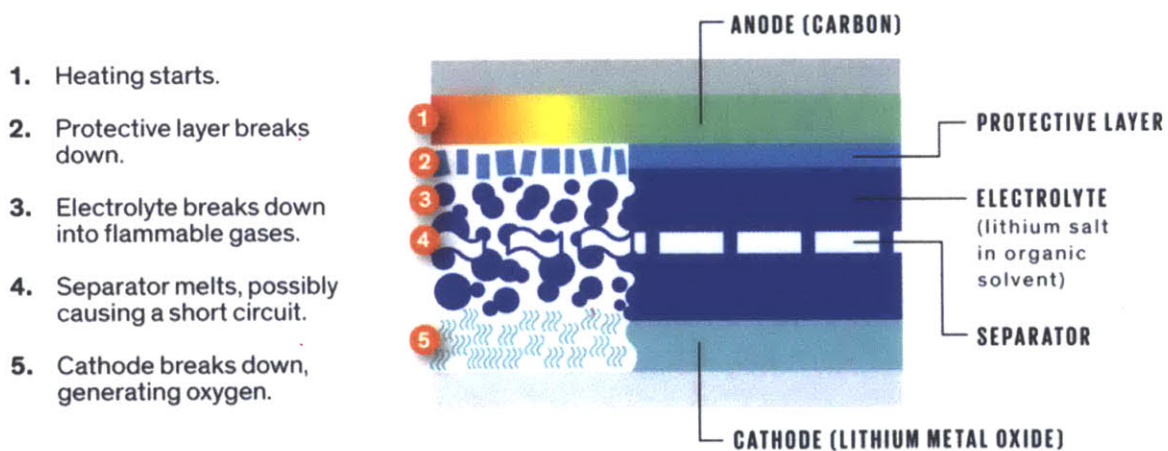SEPARATOR

CATHODE (LITHIUM METAL OXIDE)

Figure 6: A diagram of what happens to a lithium ion cell during thermal runaway (source: ieee.org)

At this point the pressure inside the cell is extremely high and the cell ignites and explodes catastrophically and dangerously. Of course, this does not happen every time a cell overheats. Sometimes the cell's safety features work properly and keep

the cell from completing this thermal runaway cycle [12]. Other times the cell will rupture earlier, releasing the gas and the pressure and stopping the further heat buildup before the cell can ignite. Still, each of these steps in the thermal runaway process damages the cell and also has the potential to cause neighboring cells in the pack to overheat. A temperature rise in a single cell can therefore start a domino effect and cause an entire pack to enter thermal runaway and fail catastrophically [13]. Figure 6 shows a picture of what happens during thermal runway.

These failures are especially dangerous because lithium-fires are difficult to contain and put out [14]. Lithium cells are also found in devices as small as cell phones to vehicles like cars and planes. Many significant failures have been recorded in the last several years. In the summer of 2006 a Sony manufacturing error, coupled with high outside temperatures, caused a number of significant failures (among others a laptop battery in the overhead compartment of a plane waiting on the tarmac in Chicago overheated and caught fire and another exploded during a business meeting in Osaka) [14]. More recently were the highly public Boeing 787 battery failures [15]. Lithium ion batteries do have a number of built in safety features to prevent this from happening but these features can become overwhelmed and fail. Therefore it is extremely important that the cell's temperature is controlled externally and that the pack and device are designed to dissipate heat properly so that the cells can be kept below the maximum safe temperature.

Figure 7: A laptop with a li-ion battery that caught fire (source: acousticpc.com)
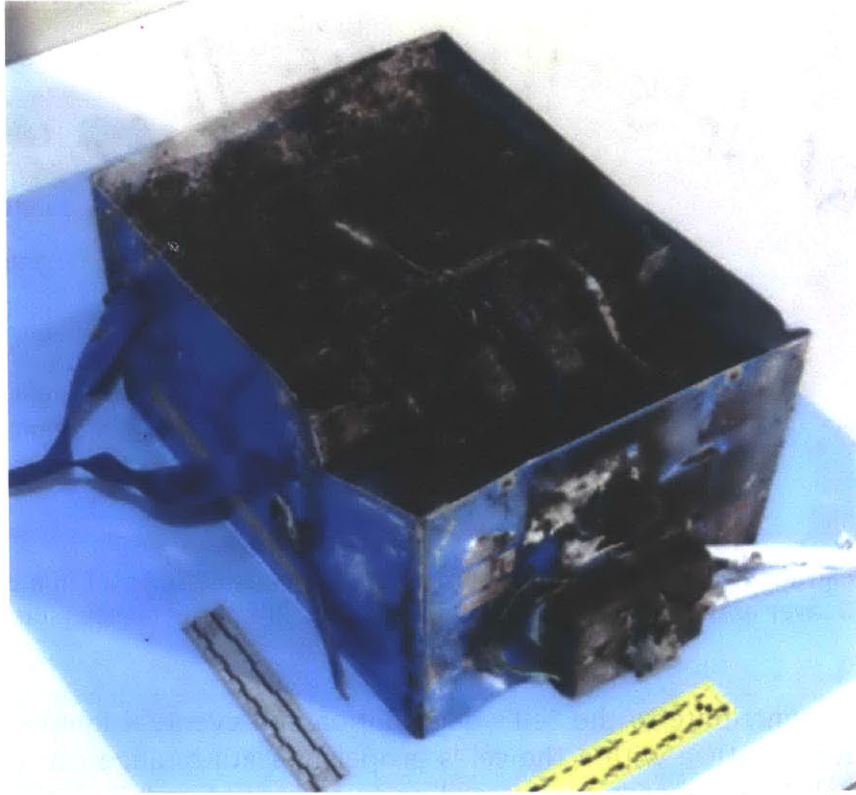
Figure 8: The auxiliary power unit from a Boeing 787 that caught fire due to thermal runaway (source: ieee.org)

3.2.2 Relation to Pack Life

Assuming the cells can be kept below this maximum temperature, packs must also be designed keeping in mind the thermal gradient (ΔT) over all of the cells. As stated above elevated temperatures increase the rate at which the reaction in the lithium-ion cell occurs and when lithium-ion cells heat up they degrade faster. This happens for two main reasons [16]. First, while the cell charges and discharges there are also a number of side reactions that go on other than the main battery reaction. These side reactions are unwanted and generally detrimental to the cell's performance. At higher temperatures; because of the Arrhenius law, these reactions happen more often and faster which leads to a loss of cycle-able lithium and a loss of active material. Second, an increase in the number of side reactions on the electrode surfaces results in faster buildup of the SEI layer there [18] [19].
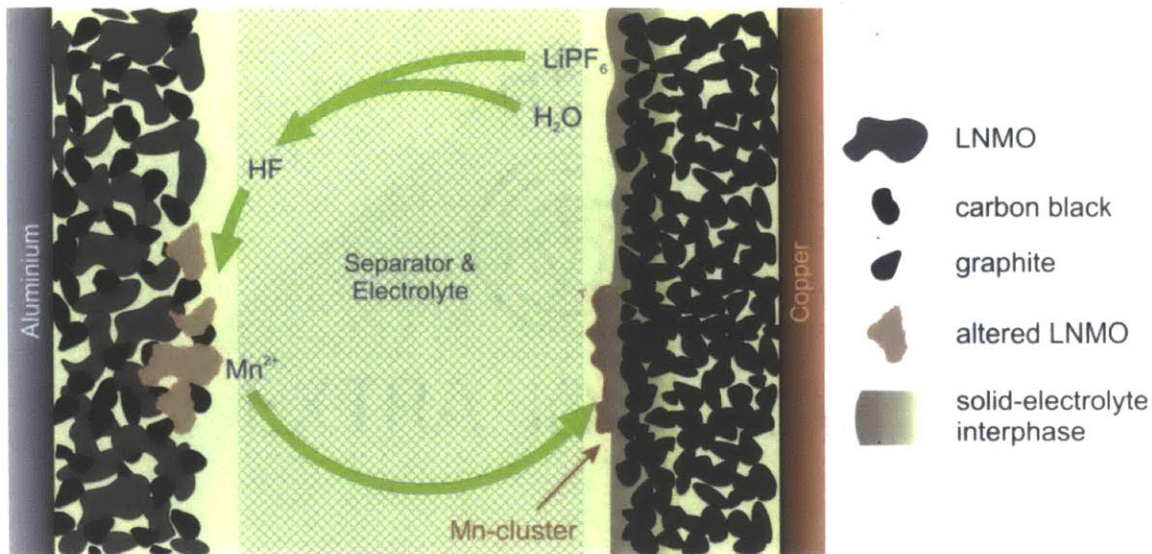
Figure 9: A diagram of a side reaction, the dissolution of manganese, in a li-ion cell that affects the SEI layer of the cell and is detrimental to the cell's performance (source: int.kit.edu)

Both of these contribute to the cell's degradation and eventual failure. Even small changes of temperature within the cell's proper operating range can lead to large changes in cell life. For example, according to Mahamud and Park the lifespan of some lithium-ion cells can be reduced by about two months for every degree of temperature rise in an operating temperature range of 30-40°C. Furthermore an automotive battery pack is considered dead when it reaches 80% of its original capacity. The pack's capacity is at any time determined by the capacity of the worst cell in the pack since each cell should be loaded with the same current. If one cell degrades faster than the other cells in the pack then when that cell dies the whole pack is practically considered dead. Therefore if even one cell in a larger pack is operating at just a few degrees higher than the rest of the pack, the entire pack could be compromised far earlier than it otherwise would be. Also considering that 30-40°C is the specified safe operating temperature range for many lithium-ion cells, it is clearly extremely important to regulate the temperature gradient, or ΔT, over the pack even within that range to ensure the pack's longevity [17].

For some packs this temperature regulation can happen with natural convection but for many packs, like in cars, an external battery cooling system is needed to keep the temperature gradient small and to keep the cells below their max operating temperature. Even with an external cooling system keeping the pack operating at a constant temperature is not as simple as it sounds. Any cooling system will have inefficiencies and will not be able to cool each cell at exactly the same rate. Most cooling systems also use one-directional flow moving from an inlet to an outlet. This automatically introduces problems since in general the air at the outlet will be hotter than at the inlet, so the cells closest to the outlet will be hotter and will degrade faster [17]. Some studies have shown, however, that this may not always be true since in the flow can become turbulent and eddies and currents can form,

16

seriously complicating the air movement and significantly altering the heat transfer patterns. In this case the heat transfer is much harder to map but invariably some cells will be hotter than others. Also, as the battery pack gets larger the cooling gets more complex since there are more cells for the air to cool.

4 Test box design

4.1 Boston Power Swing Key 442

This experiment was conducted using Boston Power's Swing Key 442 lithium—ion battery block. The Swing Key is made to be a versatile building block for electric vehicle applications that can be stacked together to make a pack of virtually any size for electric bikes, scooters, cars, and hybrids. Appendix A has the Swing Key 442's datasheet. The battery is rated for a charging temperature range of -20 to 60°C and a discharge temperature of -40 to 70°C. It has an energy density of 171 Wh/kg and a capacity of 42Ah.
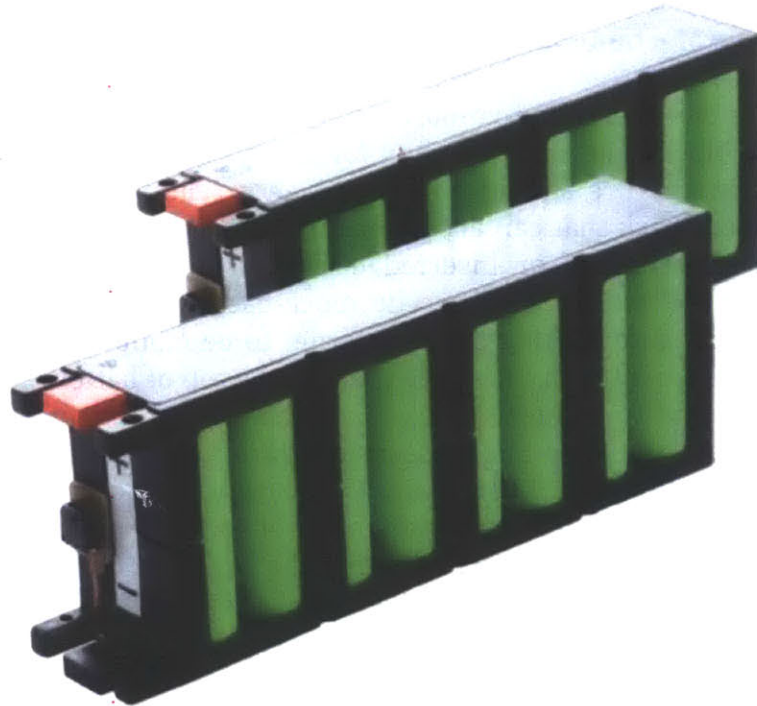
Figure 10: The Boston Power Swing Key 442 lithium-ion battery block used for this experiment (source: boston-power.com)

Since the Swing Key is a building block for modular battery packs it is very important to understand generally how the blocks will heat up during operation. The purpose of this experiment was to determine the temperature gradient and characteristics of Swing Key packs of various sizes (between one and ten blocks stacked together) with and without unidirectional cooling airflow. To accomplish this a test setup was needed that could reliably cycle (discharge and charge) the

Swing Key battery blocks so that they could heat up and their temperatures could be recorded.

4.2 Battery Cycler Options

There are commercial battery cyclers available that would have allowed us to perform the testing we wanted. Early on in the project quotes were solicited from Maccor, Aeronvironment and Chroma who make such systems. All of the cyclers they offered that would have accomplished the task were upward of $50,000 and thus too expensive to be used for our purposes. Therefore, in order to perform the battery cycling it was necessary to design and build our own equipment.

In order to accomplish the experiment, a testing box was designed with mechanical and electrical subsystems. The testing box could accommodate and test anywhere from one to ten Swing Key blocks stacked on top of each other, much like they would be in an electric vehicle battery pack. The box was designed to allow for instrumentation and cooling of the blocks and also had to be fire resistant.

4.3 Battery Cycler Mechanical Design

The testing box is designed in a two-part structure. There is an inner acrylic box to hold the battery blocks and an outer box for safety to prevent short circuits and attempt to contain any fire should one start. The acrylic box is built to be like a configurable battery pack that can accommodate anywhere from one to ten blocks. The blocks can be removed or inserted easily so that a large variety of pack configurations can be tested. This acrylic mock-battery-pack was built of easily changeable, laser-cut, interlocking pieces in order to be modular and accommodate changes in the experiment plan down the road. At the top of battery pack there is an adapter plate that fits to a duct system. The duct system is connected to a fan, mounted on the outside of the box as seen in Figure 12, that was used to cool the batteries during some of the experiments. The battery pack and duct system were sealed as well as possible with foam gasket material and duct tape to ensure that the flow was directed only onto the pack and that the pressure drop measured would accurately show the pressure drop over the pack.

As is always the case when cycling li-ion batteries, care had to be taken to ensure that the setup was safe and could effectively contain a fire should a cell overheat during testing. As such, the outer box is designed with fire safe materials to contain any fire that might start should one of the cells rupture. The bottom of the box is lined with high-temperature ceramic tiles while the box itself is made from fire-resistant MDF. The whole box is mounted on wooden struts that are mounted on casters for extra mobility and there is a shelf just above the casters for storage.

Figure 11: CAD renderings of the mock battery pack with Swing Key blocks inserted. The right image is a zoomed in version of the top of the left image
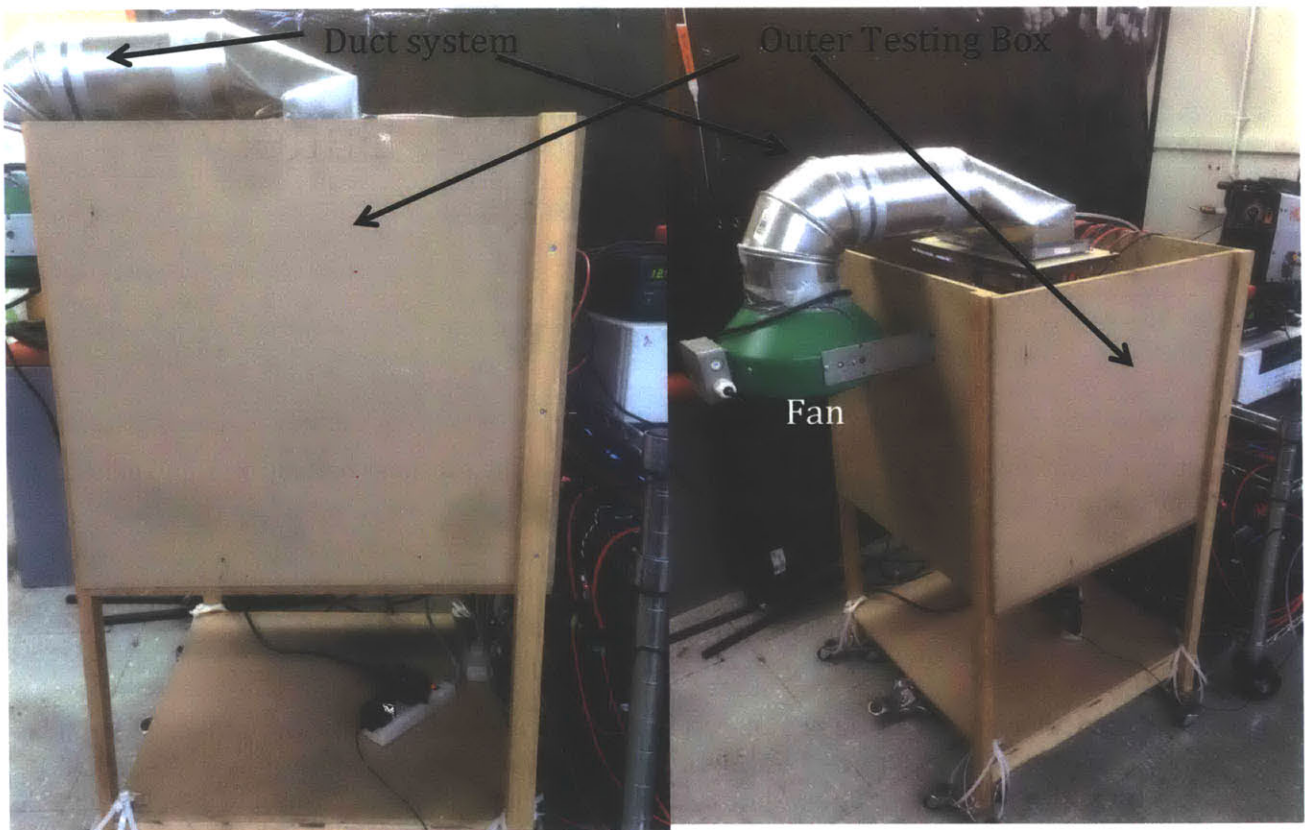

Duct system   Outer Testing Box

Fan

Figure 12: The outer test box with attached fan and duct system
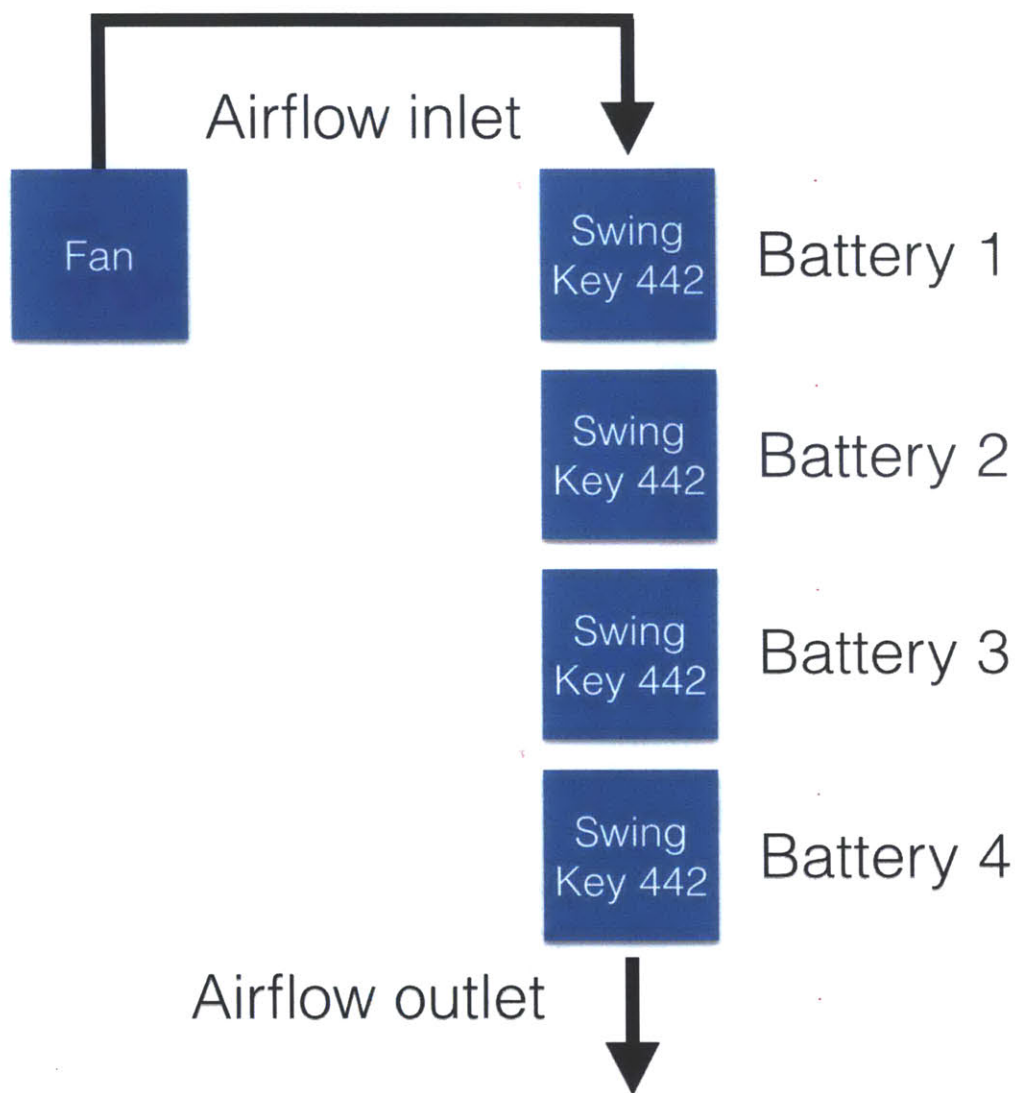
Figure 13: Airflow diagram. The air entered the pack at the top, near battery one, and exited at the bottom, near battery four.

4.4 Battery Cycler Electrical Design

4.4.1 The Power System

The electrical system can be broken up into two main subsystems, the power system and the sense system. Figure 14 shows a block diagram of the main power electrical system for the test setup. The Swing Key battery packs charged from and discharged into four Ultrapower EV31 12-volt batteries. These batteries were chosen for their high capacity and cost effectiveness. The charge and discharge rates were controlled using a combination of 20 Powerlab 8 and Powerlab 6 battery cyclers. The Powerlab

8 and Powerlab 6 have no differences significant to this test and will hereby be referred to as 'Powerlab.' The Powerlab is a hobby battery cycler that is capable of charging and discharging a battery at a maximum current of 40A. The Boston Power cells were to be charged and discharged at a 2C rate. This meant that a charge and discharge current of around 80A was needed since the batteries have around an 80Ah capacity. Since each Powerlab could only handle 40 amps, two Powerlabs were connected in parallel to each Boston Power cell. Unfortunately, I was unable to successfully run two Powerlabs at the same time on each Boston Power cell because of internal controls in the Powerlabs preventing them from operating while connected in parallel. As such the experiments were all conducted at 1C.
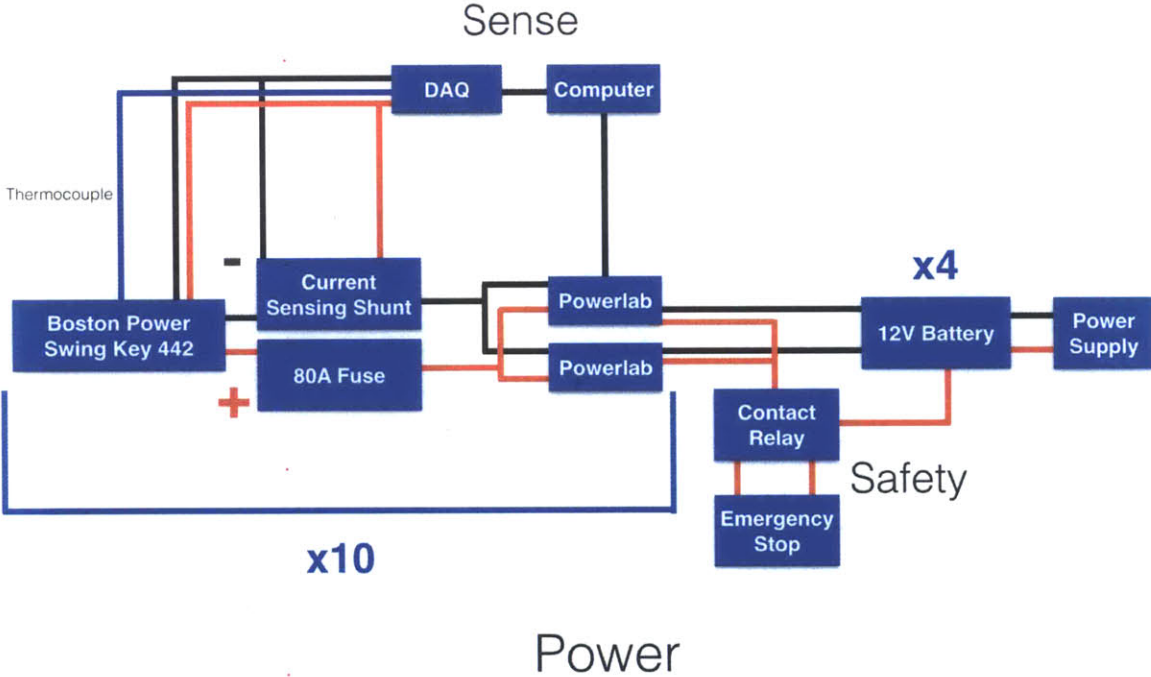
Figure 14: Block diagram of the main electrical system. Each of the Swing Key blocks was connected to two Powerlab battery cyclers through an 80A fuse on the positive side and a current sensing shunt on the negative side. The Powerlabs were connected to the 12V batteries through a contactor and emergency stop so that power could be cut off quickly in the event of an emergency

As shown in the block diagram, each Swing Key block was connected to the Powerlabs through an 80A fuse on the positive side and a shunt on the negative side. The fuse was connected as close to the Swing Key positive terminal as possible. The 80A fuse was to mitigate risk of short circuiting the batteries during assembly and testing. Such a large fuse was necessary because I expected to be charging the batteries with a maximum current of 80A. The shunt had a very low, known resistance and was used for current sensing. The Powerlabs were connected through a USB hub to a computer that was used to monitor and control them throughout the test. They were connected directly to the 12V batteries on the

21

negative side and on the positive side through a relay and emergency stop. The batteries were all connected in parallel with a BK Precision 1900 switching mode power supply that was capable of sourcing 60A at a maximum voltage of 16V. This was to ensure that while charging the Swing Key blocks the 12V batteries would never discharge too low and to ensure that the four 12V batteries would all remain at the same voltage when charging and discharging.

Figure 15: A Powerlab battery cycler

Wire gauges and connector sizes for the entire power side system were found using the 2C (80Ah) discharge rate. Assuming that each Powerlab had to deliver 40A, 10awg wire was used to connect the Powerlabs to each other. Since each Swing Key block had to charge or discharge using 80A, 6awg wire was used to connect the blocks to the Powerlabs. 6awg wire was also used to connect the 12V batteries to each other and do the power supply.

4.4.2 The Sense System

The sense side system's main data acquisition module was an Agilent 34980A Multifunction Switch/Measure Unit that was connected to the computer. It was

chosen because of its capability to monitor up to 40 channels and to interface with the computer for data storage. The DAQ monitored a large number of inputs for every test. First, it monitored the temperature of each cell with a type-J thermocouple. Each thermocouple was bolted onto its Swing Key's negative terminal.

While the Powerlabs do have current and voltage sensing capabilities, they had to sit on a cart next to the battery cycling box and as such were wired fairly far away from the actual batteries. Because of this, when the batteries were charging or discharging, and a current was applied, the voltage readings given by the Powerlabs were not accurate due to the voltage drop across the wires. To get an accurate voltage reading, 22awg sense wires were connected directly to the positive and negative terminals of the battery and fed into the DAQ. This ensured an accurate voltage reading at all times during the test.

As mentioned above, each Swing Key block's negative terminal was wired to the Powerlabs through a shunt of low, known resistance (shown in Figure 18). The voltage across the shunt was read into the DAQ with two more 22awg sense wires connected to the screw terminals shown in the picture. With this voltage and the known resistance it was possible to find the current across the battery at any given time to confirm that the battery was charging or discharging at the rate that the Powerlab said it was.
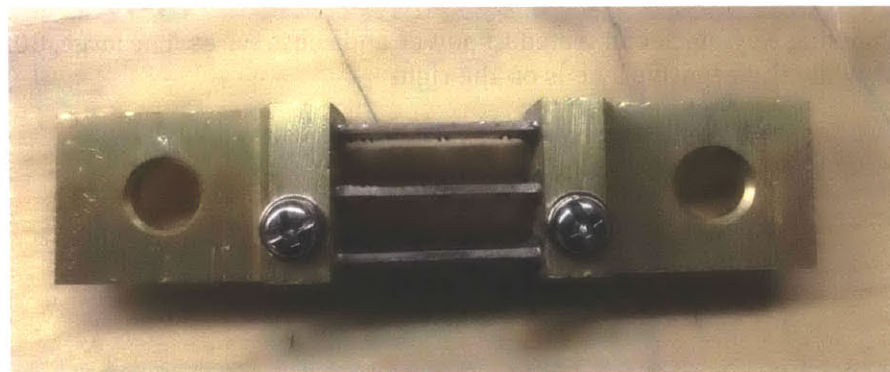

Figure 16: One of the shunts used for current sensing. The two screw terminals were connected to sense wires from which a voltage was read by the DAQ. The voltage could easily be converted to the battery's current because the resistance of the shunt was known (0.00024 ohms).

For tests where the pack was fan cooled, the air flow over the pack was monitored using a handheld Amprobe TMA-21HW hot wire anemometer. Measurements were taken above the pack, in the duct system, and at the bottom of the pack under all of the battery blocks. The air flow measurements were taken at the beginning of the experiment and were assumed to be constant throughout. The pressure drop over the pack was monitored with a Panasonic DP2-41 digital manometer. The manometer was connected to a fitting in the duct system just above the pack (shown

23

in Figure 20). The pressure was read there and the pressure at the bottom of the pack was assumed to be ambient.
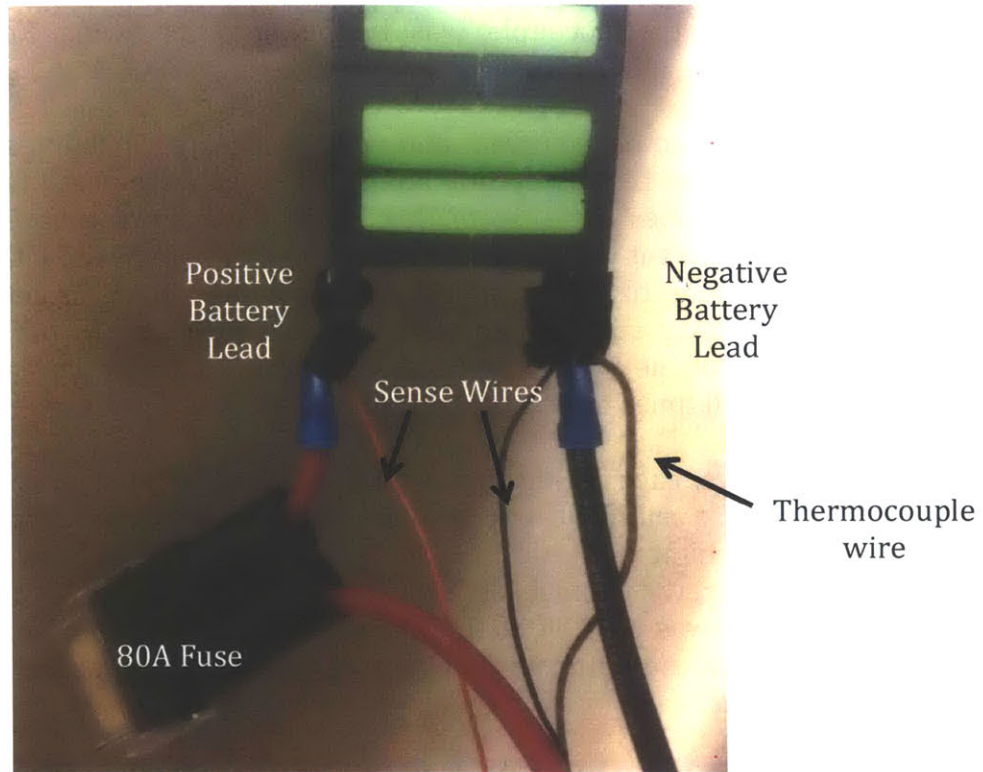

Figure 17: Swing Key block connected to power and sense wires. The large, 80A fuse is seen on the left while the negative lead is on the right
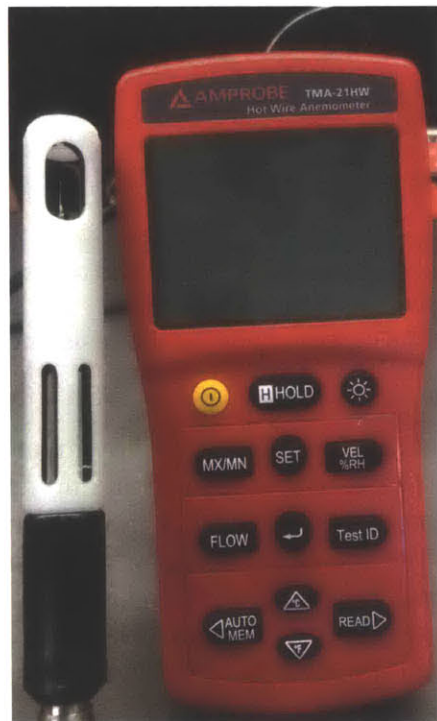
Figure 18: The handheld hot wire anemometer used for measuring airflow over the pack. Measurements were taken before the test at the top and bottom of the pack and were assumed to be constant over the test

Figure 19: The manometer used for measuring airflow over the test and the place in the duct system where the pressure was measured
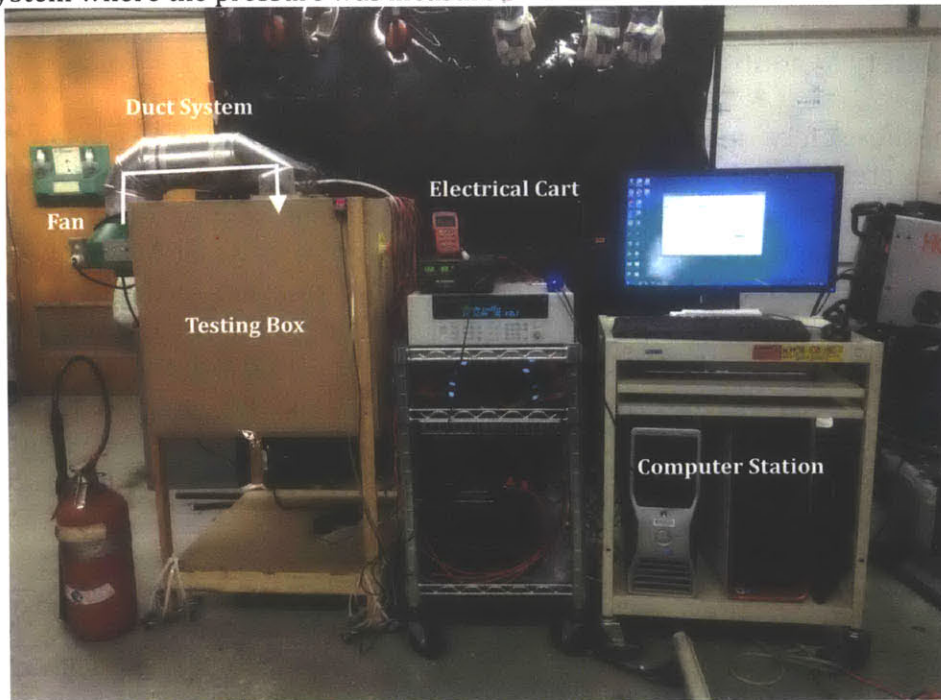
Figure 20: The full test setup. The testing box is on the left, the electrical cart in the middle and the computer station on the right. Arrow shows direction of airflow onto the batteries.
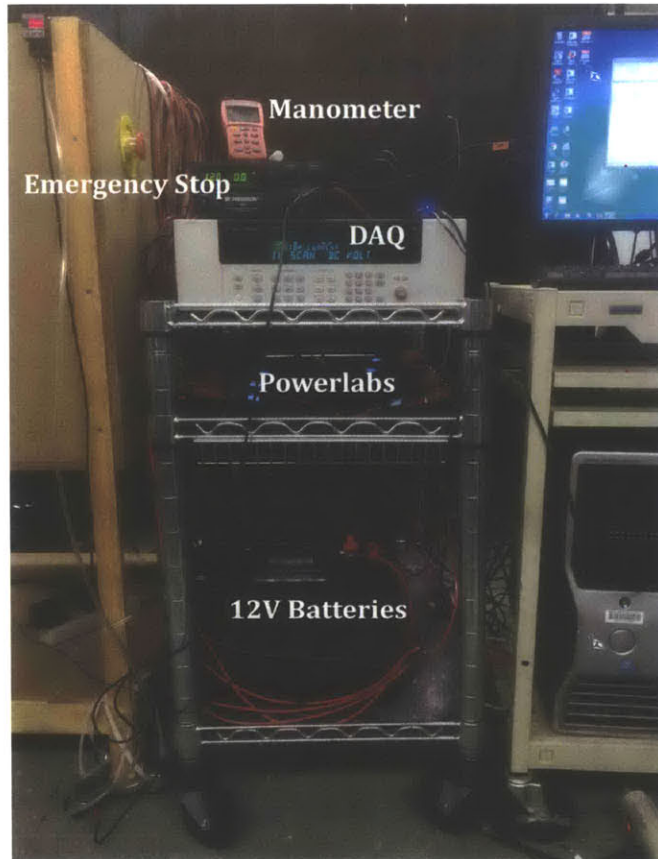
Figure 21: The electrical cart.

4.4.3 The Safety System

Even with the safety mechanisms built into the Swing Key batteries, it was important to create a safe test system since, as described above, thermal runaway could still occur while cycling leading to catastrophic failure of the cells and significant damage to equipment and people near the test setup. As mentioned above, for safety purposes the Powerlabs were all connected to the 12V batteries through a contactor. An emergency stop button that could cut off power to the Powerlabs at any time controlled the contactor. This ensured two things. First: when the button was pressed I knew the system was off and I could leave the room safely without worrying that a battery was still charging. Second: in the event of an emergency I could very quickly cut the power, stop the charge or discharge cycle and prevent as much further damage and danger as possible.

In addition, an operator was by the test setup at all times while it was running, monitoring the temperature, voltage and current of the cells with the DAQ to check that they were not entering an unsafe region. All connections were also checked before and after each test to make sure no leads had been crossed that shorted the batteries. Furthermore, for when the test setup was off, a Wi-Fi connected smoke alarm was placed in the test box so that if a fire broke out while no one was in the room I could receive an alert and notify emergency services.
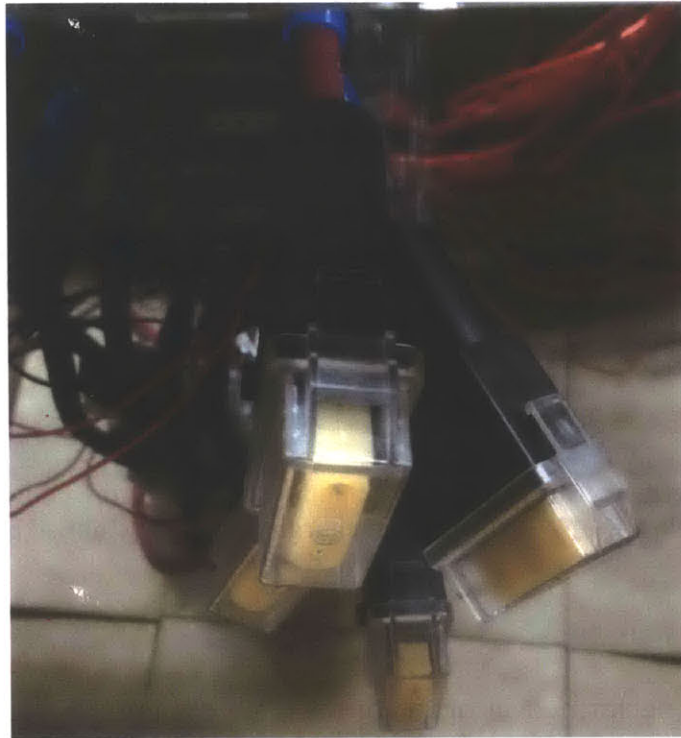
26

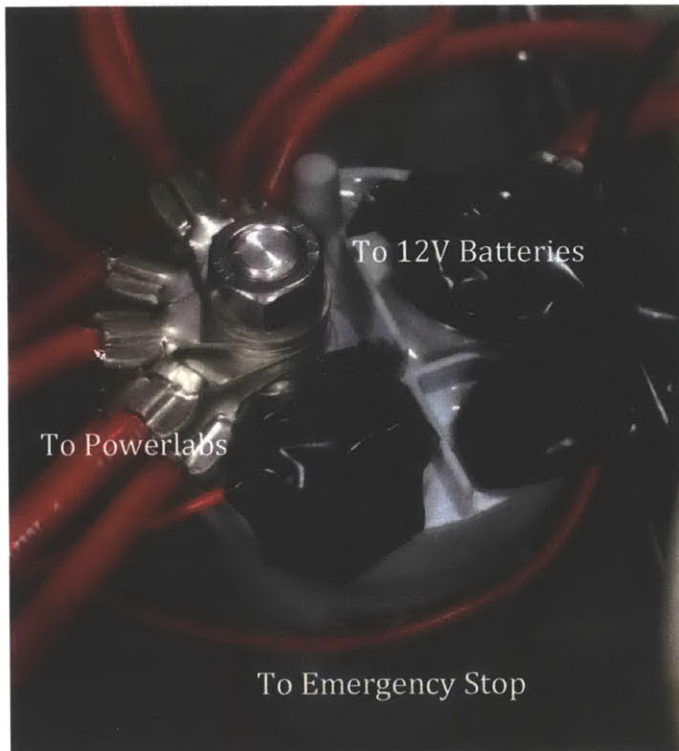Figure 22: Four 80A fuses connected to the Swing Key blocks in the test setup

Figure 23: The contactor with wires that connect it to the Powerlabs, the 12V batteries and the emergency stop switch
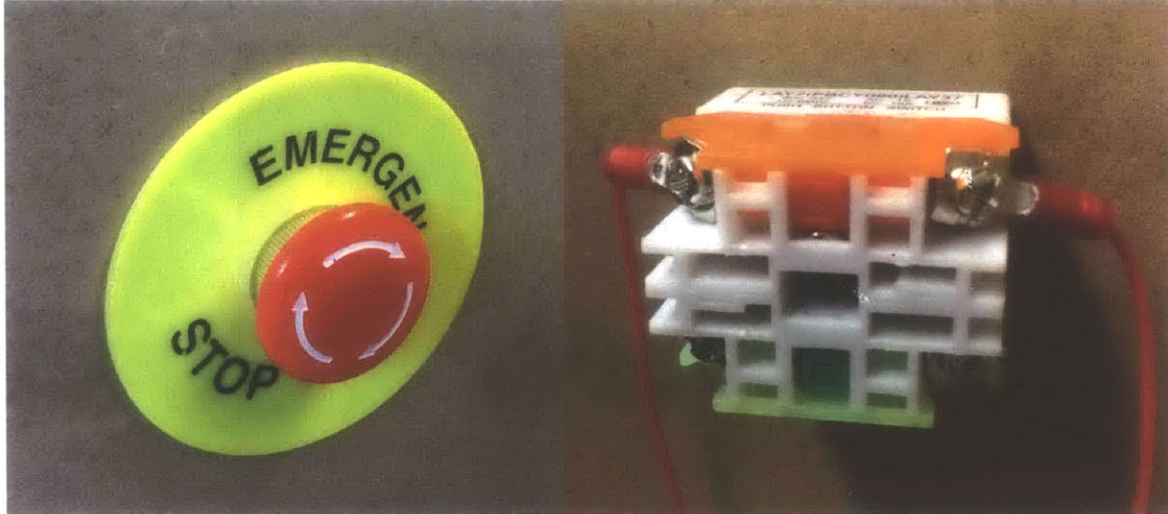
Figure 24: The emergency stop button, front and back. This button allowed for quick and safe shutoff of the Powerlabs to ensure that charging could be stopped quickly in the event of an emergency

5 Results and Discussion

Eight tests were performed in order to determine the temperature gradients of a battery pack during operation. Batteries were cycled, discharged then charged, in packs of one, two, three and four, with and without air-cooling. The air-cooling was provided by the fan built into the test setup and was kept constant at around 0.2 m/s at the top of the top of the pack. The battery pack was always loaded from the top; the test with one battery had the battery in the top slot, the test with two batteries had them in the top two slots etc. The tests were all performed at approximately a 1C rate or, in other words, they were charged and discharged at a current of 40A. The batteries were charged to around 85% capacity and discharged to around 30%. Voltage, current and temperature data was taken at a rate of one sample per second. Each experiment took from one and a half to two hours to complete. The current and voltage data from all eight tests is displayed in Appendix B.

Unfortunately, the battery cycling could not be synced perfectly between batteries since all started at slightly different charge levels and took slightly different times to charge and discharge. The tests could also not be started at exactly the same time since the Powerlabs were each controlled by different instances of the software and had to be started one after the other. Still, everything possible was done to ensure that the batteries stayed at approximately the same point in the cycle and the cycles were always within a couple minutes of each other. All battery temperature data has been synced with the battery's charge time to match up the charge and discharge cycles between batteries in an experiment.

Also, the Powerlabs have a setting that controls the 'cool down' time between charge and discharge for the batteries. During the time the current to the batteries is cut off

and they neither charge nor discharge. As such their temperature decreases. For some of the Powerlabs in some of the experiments this cool down time was set to one minute, while for most Powerlabs it was set to five minutes. This was a mistake and caused some small discrepancies in the data that can be seen in the figures below. This did not, however, affect the outcome of the tests. The full results for the tests are shown in Table 1.

Table 1
Compiled Results from All Eight Tests

Configuration	Inlet Average Flow Rate [m/s]	Outlet Average Flow Rate [m/s]	C Rate	Pressure Drop [psi]	Approximate ΔT [°C]	Peak Temperature [°C]
1 Block	No Flow	No Flow	1	N/A	N/A	35.9
1 Block	0.2	Not taken	1	0.04	N/A	27.5
2 Blocks	No Flow	No Flow	1	N/A	0.4	38.5
2 Blocks	0.22	3.9	1	0.04	1.4	30.1
3 Blocks	No Flow	No Flow	1	N/A	2.5	42.6
3 Blocks	0.27	3.1	1	0.06	1.9	31
4 Blocks	No Flow	No Flow	1	N/A	3.0	43.4
4 Blocks	0.21	2.9	1	0.06	2.9	34.5

The results from the tests conducted with a single battery block are graphed in Figure 25. For both lines, and for all graphs shown below, the initial upward slope indicates the discharge part of the cycle, the subsequent downward dip is the aforementioned cool down period and the second upward slope is the charge half of the cycle. The drop off at the end is the time after the test finished before data acquisition was stopped. Also for all tests, battery 1 is the uppermost block, closest to the cooling fan, and the subsequent batteries are lower in the pack. In Figure 25, the red line shows the test done without any air-cooling and the blue line shows the test down with cooling. The green line shows the ambient temperature. This result confirmed that the air-cooling system worked since the uncooled battery was significantly warmer than the cooled battery. The maximum temperature reached by the uncooled battery was 35.9°C while the maximum temperature reached by the cooled battery was 27.5°C.

For all tests the temperature rose very quickly at the very beginning of the test then settled to an approximately linear steady state increase rate. This is because at the beginning of the test the battery had to dissipate heat from a sharp increase in current, and as the current rose the temperature rose. Once the battery settled into its charging or discharging current the temperature then increased proportionally to the heat dissipated by the battery and rose linearly.
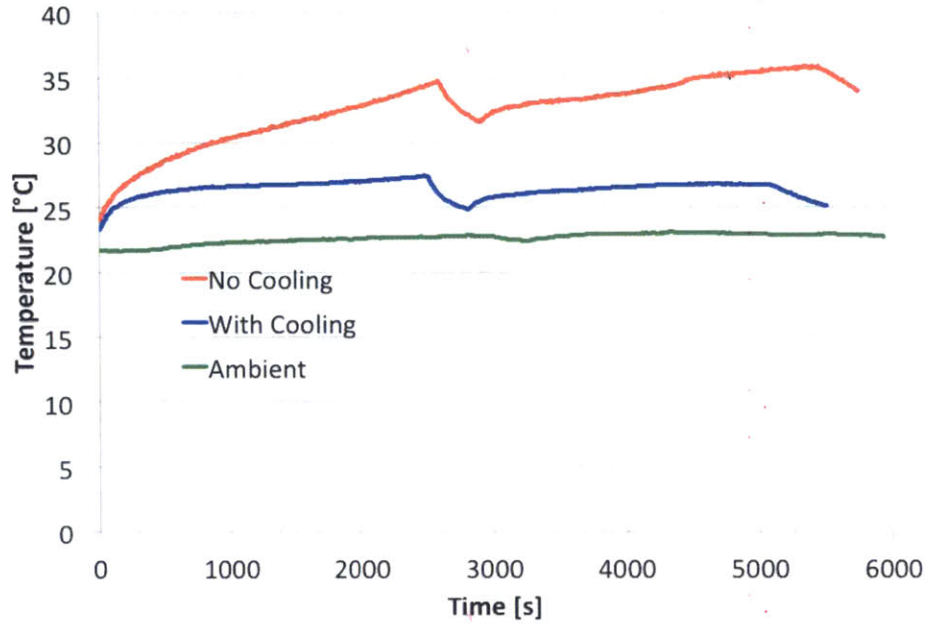
Figure 25: Results from the two tests, cooled and uncooled, with a single battery block. The red line is the uncooled test while the blue line is the cooled test and the green line is the ambient temperature. The cycle starts with a discharge, has a brief period of no current then finishes with a charge. The uncooled test is significantly warmer than the cooled test, as expected

The results from the tests with two battery blocks are shown in Figure 26. The temperature difference in the uncooled test can be attributed to the problem of different cool down times mentioned above. In the cooled test, however, the lower battery is clearly hotter than the upper battery in the discharge, and in the charge, even though it has a longer cool down time, still heats up more than the upper battery. The maximum temperature reached by the upper block was 28.8°C while the maximum temperature reached by the lower block was 30.2°C. This difference becomes more pronounced in the tests with three (Figure 27) and four (Figure 28) batteries. In Figure 27, the three block test, for the cooled test the second and third blocks are around the same temperature throughout the test while the uppermost block remains about 1°C cooler. In the uncooled test there is also a gradient, this time the lower block is the coolest while the middle block is the hottest. This is likely because the lower block had more surface area open to the air while the middle block was sandwiched by the other two batteries. The rate of convective heat transfer for natural convection is given by the equation

$$Q^{\bullet}{}_{conv} = hA(T_s - T_\infty)$$

where $Q^{\bullet}{}_{conv}$ is the rate of convection, h is the heat transfer coefficient, A is the area over which the convection occurs, T_s is the temperature of the hot surface and T_∞ is the temperature of the convective air. In the case of the middle battery, the convective air cooling it was trapped between and heated by the two batteries

30

above and below it and had little opportunity to be replenished by cool air from outside the test box. This made T_∞ hotter, causing there to be less heat transfer away from the middle battery and thus keeping it hotter. The top battery had one side open to the air inside the duct system and, although this air was more or less sealed in the ducts and was heated by the batteries' operation, it was a larger volume and had more opportunity to be cooled by the ambient air in the room. The lowest battery had a side open to the volume of air in the box that was completely open to the room, making its T_∞ lowest and allowing it to be cooled the most. In the cooled four block test the unsynchronized cool down time issue was fixed. In this test there is a clear correlation between how low in the pack the battery is and how hot it gets. Maximum temperatures for each cooled battery during charge and discharge for the four-battery test are shown in Table 2.

Table 2
Maximum Temperatures During Charge and Discharge for the Four-Battery Cooled Test

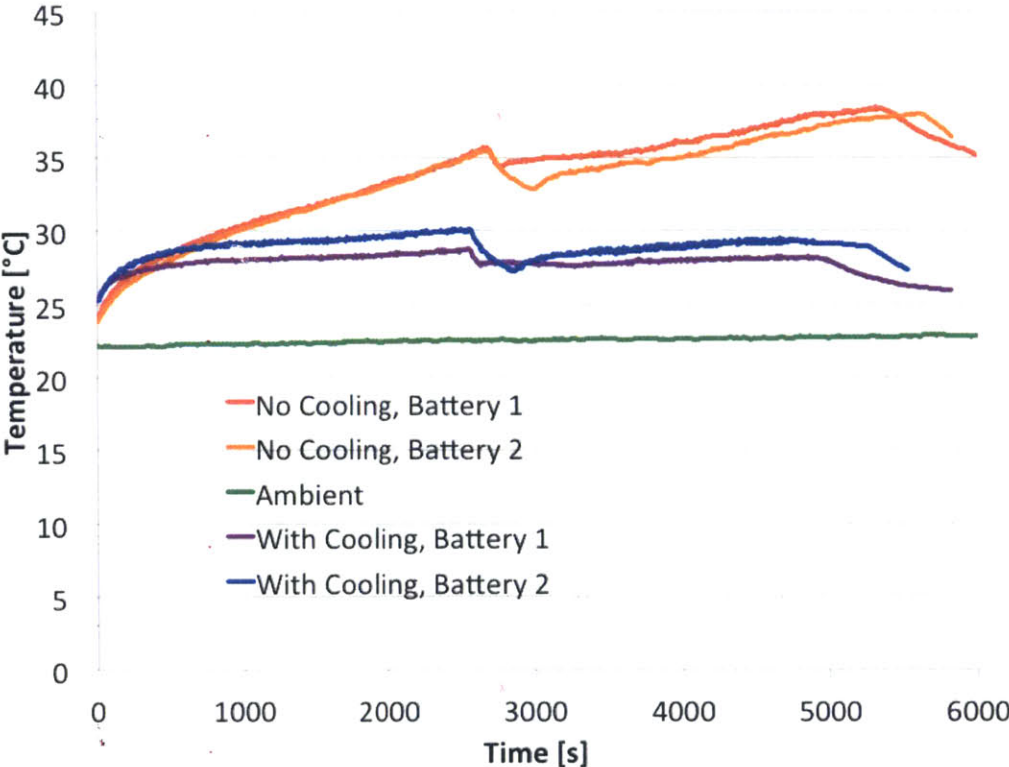|	Maximum Charging Temperature [°C]	Maximum Discharging Temperature [°C]
Battery 1	30.6	31.6
Battery 2	31.3	32.5
Battery 3	31.9	32.8
Battery 4	33.7	34.5

Figure 26: Results from the two tests, cooled and uncooled, with two battery blocks. Here the significant temperature gradient over the pack in the cooled test can already be seen

31

In the uncooled four-block test (as shown in figure a temperature gradient is again seen with the lowest battery being significantly cooler than the upper batteries. Again this is likely because it had more access to free convection to keep it cooler. For the cooled test, now that the cool down time issue has been fixed, there is a very clear temperature gradient in the pack. The uppermost block is the coolest with each subsequent block heating up more. The middle two blocks are at almost the same temperature while the lowest block is over 2°C warmer than the uppermost block throughout the test.
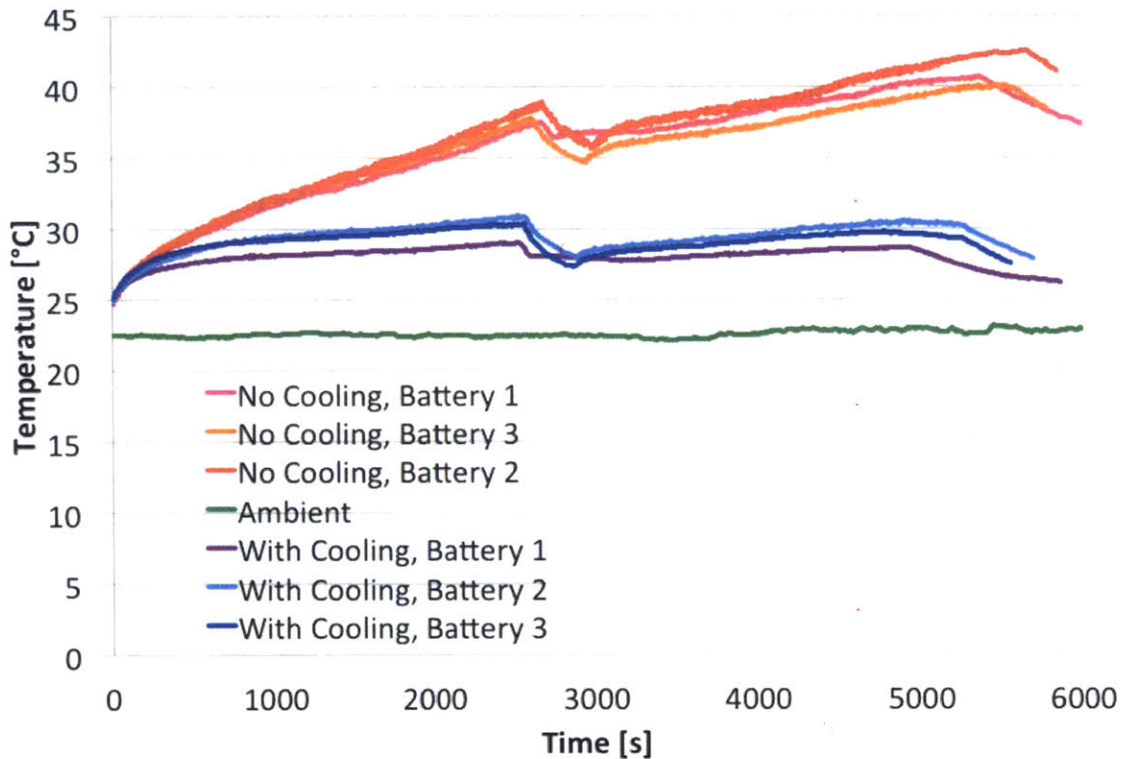
Figure 27: Results from the two tests, cooled and uncooled, with three battery blocks
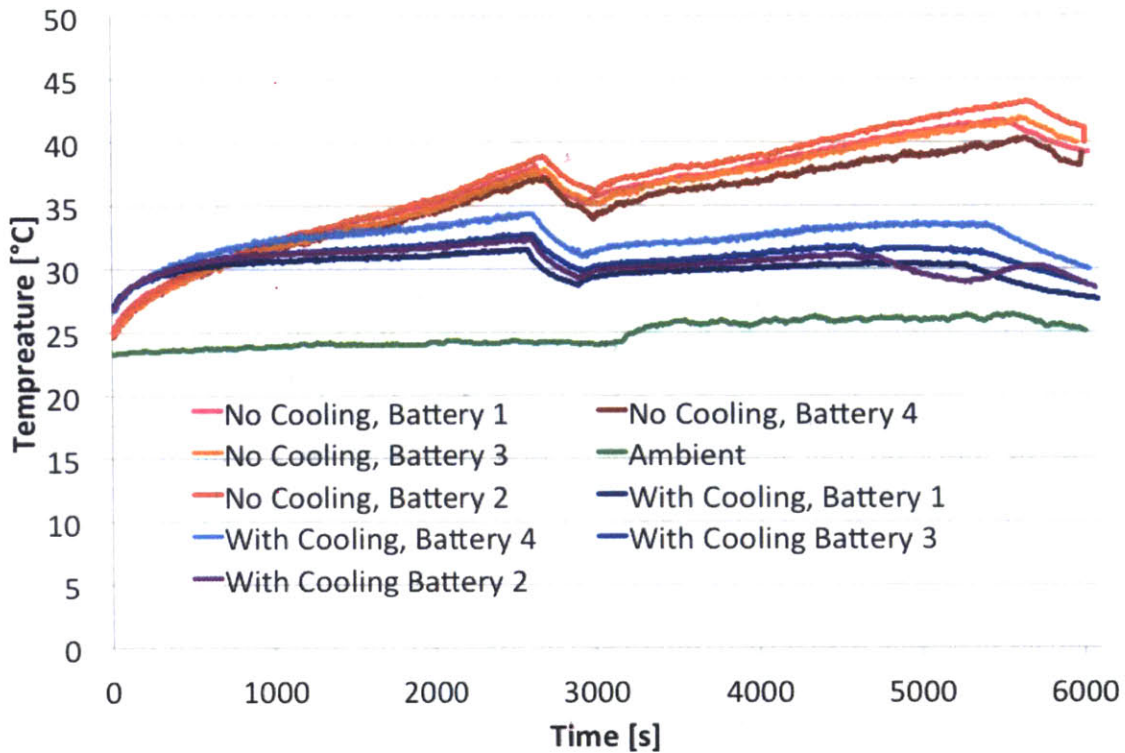
Figure 28: Results from the two tests, cooled and uncooled, with four battery blocks

These results indicate that for any size battery pack there can be significant (over 1°C) temperature gradients in the packs. According to the research cited earlier by Mahamud and Park even a 1°C gradient can decrease the life of the battery by up to two months for some cells. In the largest pack tested here the maximum ΔT was almost 3°C between the hottest and coldest cells. As shown in the results above, between the two block test and three block test the ΔT rose by 0.5°C. From the three block test to the four block test the ΔT rose by 1°C. Without further tests it is impossible to know for sure that this trend will continue with doubling the increase in pack temperature gradient for every block added to the pack. In fact, as more blocks are added the ΔT could begin to increase more slowly again. We know, however, that the heat energy gained or lost by the air is given by the equation

$$q = mC\Delta T$$

where q is the heat energy transferred to or from the substance, m is the mass of the substance, C is the substance's specific heat and ΔT is the substance's change in temperature. Assuming each battery in isolation gives off approximately the same amount of energy, and that the volume of air in the pack does not change substantially, the ΔT should vary approximately linearly. Then we can assume that the pack's temperature gradient would rise 1°C for every block added after four. Given that a 5°C ΔT over a pack is the generally accepted number for the automotive

industry, we could then build a pack with this configuration and cooling rate with no more than six blocks before we reached an unacceptable ΔT.

This significant temperature gradient sheds light on a number of design issues that need to be carefully chosen for electric vehicle battery packs. For packs this small, a reciprocating flow system, where the flow direction is reversed periodically, or a bidirectional cooling system could definitely help cool the hottest cell and would reduce the overall ΔT of the pack [17]. Still, as the pack grows, simply cooling the pack from both top and bottom might not be enough to get ride of the temperature gradient. It would certainly help to cool each cell individually with its own fan or liquid cooling agent. This is not technically practical for many battery packs however. Another potential solution is cooling the pack from the side instead of the top of the stack so that all cells receive approximately equal amounts of forced convection. This can be difficult as well, however, depending on the size and shape of the pack.

Additionally, the pack design itself should promote airflow and convection. The measured pressure drops over the packs shows why airflow between the batteries is particularly important in the case of unidirectional flow. For the one and two block packs the pressure drop was determined to be 0.04 PSI. For the three and four block packs the pressure drop was found to be 0.06 PSI. When the pressure drop increases it means the flow is having a harder time reaching the bottom of the pack. With a pack designed for easier flow from battery to battery the drop could be minimized and the forced convective currents at the bottom of the pack could do a better job of cooling it. All of these design choices could help minimize the ΔT over the pack and bring it to within acceptable levels so that the cells will age at approximately the same rate.

6 Conclusion and Future Work

In this project Boston Power Swing Key 442 battery blocks were assembled into a pseudo-EV battery pack and tested in an improvised battery cycler to determine whether temperature gradients developed between the cells while they were charging and discharging. The cells were tested in configurations of one, two, three and four batteries and with and without unidirectional air-cooling. A significant correlation was found between placement in the pack and cell temperature. The lower down in the pack, and thus the further from the outlet for the air-cooling, a cell was the hotter it became during operation. For the packs with three or four blocks there was a least a 1°C temperature rise from the uppermost cell to the middle cell(s), and another 1°C or more rise from the middle cell(s) to the lowest cell. This temperature rise is significant enough to cause a large decrease in the cell life of the hotter cells, leading to faster aging of the pack as a whole. Careful attention must be paid when designing a pack and its cooling system to minimize this temperature gradient over the pack as much as possible.

In the future it would be interesting to run these tests with different battery pack configurations to determine optimal set up for maximum air flow to all parts of the pack. It would also be interesting to run the tests with multidirectional air flow to see how much flow is needed before the temperature gradient can be brought to acceptable levels. Overall, much more research is needed to optimize the pack design for low ΔT and electric vehicle designers must take this consideration into account or risk significantly decreasing the life of their vehicle's battery packs. If they do not, fast dying battery packs will only give more reason to those who are hesitant to buy electric cars to stay with gasoline powered vehicles. It will also cause an increase in waste from electric cars as, although most batteries are recycled, the process is not 100% efficient so more and more dead batteries will be disposed of in landfills and dumps. This research has shed some light on one of the difficulties of electric pack design and can hopefully be used to better their design in the future.

Bibliography

[1] Cowan, Robin, and Staffan Hultén. "Escaping Lock-in: The Case of the Electric Vehicle." *Technological Forecasting and Social Change* 53, no. 1 (1996): 61-79. doi:10.1016/0040-1625(96)00059-5.

[2] Chan, C. C. "The State of the Art of Electric, Hybrid, and Fuel Cell Vehicles." *Proceedings of the IEEE* 95, no. 4 (2007): 704-18. doi:10.1109/JPROC.2007.892489.

[3] Smith, Meghan E. "What Percentage of Air Pollution Is Due to Cars? - HowStuffWorks." HowStuffWorks. December 07, 2010. Accessed May 06, 2015. http://auto.howstuffworks.com/percentage-of-air-pollution-due-to-cars.htm.

[4] Lu, Chris. "NGV Market Growth 2013 Analysis." CNG Tank. 2013. http://www.cng-tank.com/index.php/ngv-market-growth-2013-analysis.

[5] Steinhilber, Simone, Peter Wells, and Samarthia Thankappan. "Socio-technical Inertia: Understanding the Barriers to Electric Vehicles." *Energy Policy* 60 (2013): 531-39. doi:10.1016/j.enpol.2013.04.076.

[6] Zehner, Ozzie. "Unclean at Any Speed." IEEE Spectrum. June 30, 2013. Accessed May 06, 2015. http://spectrum.ieee.org/energy/renewables/unclean-at-any-speed/.

[7] Committee on Health, Environmental, and Other External Costs and Benefits of

   Energy Production and Consumption; National Research Council. *Hidden*

   Costs of Energy: Unpriced Consequences of Energy Production and Use.

   Washington, D.C.: National Academies Press, 2010.

[8] Conca, James. "Are Electric Cars Really That Polluting?" Forbes. July 21, 2013.

   Accessed May 06, 2015.

   http://www.forbes.com/sites/jamesconca/2013/07/21/are-electric-cars-

   really-that-polluting/.

[9] Bossche, Peter Van Den, Frédéric Vergels, Joeri Van Mierlo, Julien Matheys, and

   Wout Van Autenboer. "SUBAT: An Assessment of Sustainable Battery

   Technology." *Journal of Power Sources* 162, no. 2 (2006): 913-19.

   doi:10.1016/j.jpowsour.2005.07.039.

[10] Daniel, Claus. "Materials and Processing for Lithium-ion Batteries." *Jom* 60, no.

   9 (2008): 43-48. doi:10.1007/s11837-008-0116-x.

[11] "Prevent Thermal Runaway Propagation." AllCell Technologies. Accessed May

   06, 2015. https://www.allcelltech.com/index.php/technology/pcc-

   thermal-management/prevents-thermal-runaway.

[12] Spotnitz, R., and J. Franklin. "Abuse Behavior of High-power, Lithium-ion Cells."

   Journal of Power Sources 113, no. 1 (2003): 81-100. doi:10.1016/S0378-

   7753(02)00488-3.

[13] "Battery and Energy Technologies." Lithium Battery Failures. Accessed May 06, 2015. http://www.mpoweruk.com/lithium_failures.htm.

[14] Hockenberry, John. "Building a Better Battery" Wired 14.11: Building a Better Battery. November 2006. Accessed May 06, 2015. http://archive.wired.com/wired/archive/14.11/battery.html.

[15] Wingfield-Hayes, Rupert. "Boeing 787 Aircraft Grounded after Battery Problem in Japan - BBC News." BBC News. January 14, 2014. Accessed May 06, 2015. http://www.bbc.com/news/business-25737515.

[16] Pesaran, Ahmad, Shriram Santhanagopalan, and Gi-Heon Kim. *Addressing the Impact of Temperature Extremes on Large Format Li-Ion Batteries for Vehicle Applications (Presentation), NREL (National Renewable Energy Laboratory)*, March 11, 2013. Accessed May 6, 2015. http://www.nrel.gov/docs/fy13osti/58145.pdf.

[17] Mahamud, Rajib, and Chanwoo Park. "Reciprocating Air Flow for Li-ion Battery Thermal Management to Improve Temperature Uniformity." *Journal of Power Sources* 196, no. 13 (2011): 5685-696. doi:10.1016/j.jpowsour.2011.02.076.

[18] Arora, Pankaj. "Capacity Fade Mechanisms and Side Reactions in Lithium-Ion Batteries." *Journal of The Electrochemical Society* 145, no. 10 (1998): 3647. doi:10.1149/1.1838857.

[19] Tang, Maureen Han-Mei. (2012). Side Reactions in Lithium-Ion Batteries. UC Berkeley: Chemical Engineering. Retrieved from:

https://escholarship.org/uc/item/331948fw

[20] Erb, Dylan. "Optimization of Blended Battery Packs." DSpace@MIT:. 2013. Accessed May 07, 2015. http://hdl.handle.net/1721.1/81601.

[21] Cobb, Jeff. "Top 6 Plug-In Vehicle Adopting Countries - 2014 - HybridCars.com." HybridCarscom Top 6 PlugIn Vehicle Adopting Countries 2014 Comments. February 18, 2015. Accessed May 14, 2015.

http://www.hybridcars.com/top-6-plug-in-vehicle-adopting-countries-2014/.

[22] Tencer, Daniel. "World's Car Population Hits 1 Billion." The Huffington Post. February 19, 2013. Accessed May 14, 2015.

http://www.huffingtonpost.ca/2011/08/23/car-population_n_934291.html.

[23] "Hybrid and Electric Vehicles Struggle to Maintain Owner Loyalty, Reports Edmunds.com." Edmunds. April 21, 2015. Accessed May 14, 2015. http://www.edmunds.com/about/press/hybrid-and-electric-vehicles-struggle-to-maintain-owner-loyalty-reports-edmundscom.html.

Appendix A

Swing Key® 442 Lithium-ion block

Boston-Power's Swing Key 442 block is a high performance lithium-ion rechargeable battery with industry leading safety, energy density and long cycle life, making it an ideal energy storage solution for battery electric vehicles, e-bikes, e-scooters and plug-in hybrid electric vehicles.
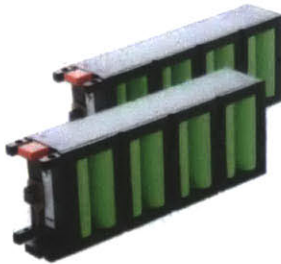
Swing Key 442 blocks are a standard battery "building block" for electric vehicles that combine the advantages of small cells with large format cells and deliver:

- Unparalleled system safety
- Cost-effective thermal management
- Common hardware compatible with next-gen capacity
- Ease of implementation

They form the foundation for our Swing RESS™ (Rechargeable Energy Storage System), demonstrated in multiple vehicle applications today.

Certifications
UN 38.3 (cell and block), UL1642 (cell)

Specifications[1]

|		Swing Key 442
Configuration		8 Parallel, 1 Series
Nominal capacity		42Ah
Nominal energy		155Wh
Nominal voltage		3.65V
Energy density	Gravimetric	171Wh/kg
	Volumetric	329Wh/L
Cycle life to 80% capacity		~2000 cycles @ 90% DOD
Standard charging method CC/CV (Constant Current/Constant Voltage)		29.4A to 4.2V
Operating voltage range		2.75V to 4.2V
Maximum continuous discharge[2]		70A
Peak pulse discharge (10s)[2]		176A
Nominal Impedance (1kHz)		2.65mΩ
Nominal module weight		0.90kg
Operating temperature	Charge	-20 to 60°C
	Discharge	-40 to 70°C
Storage temperature[3]		-40 to 60°C

[1] Testing performed at 25°C and C/5 discharge. Specification subject to change.
[2] Requires active thermal management.
[3] Contact Boston-Power for specifics on operation and storage at temperature extremes.

Dimensions & Terminal Locations

40

Discharge curve

Charge Curve
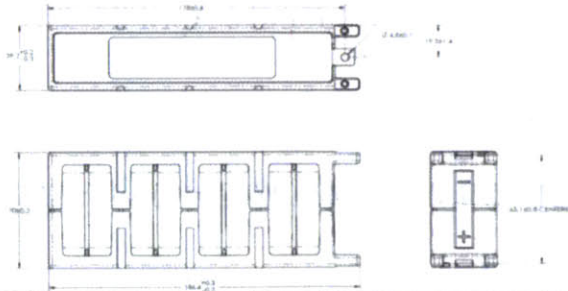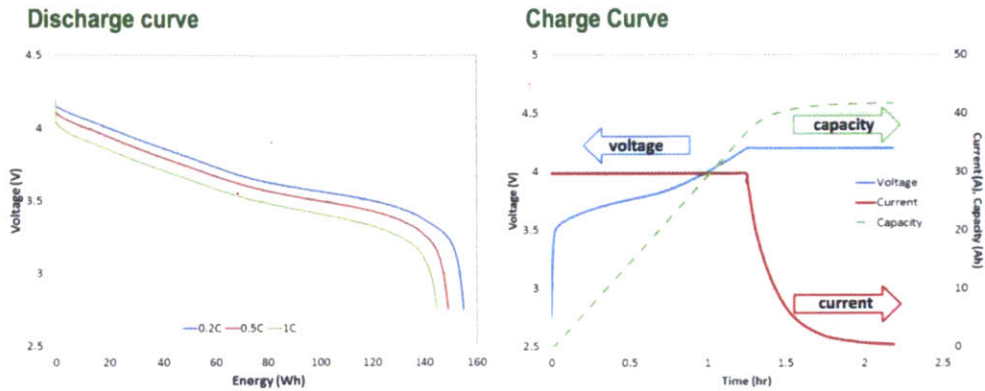
Applications: This block is targeted for use in:

- Battery Electric Vehicles
- Plug-In Hybrid Electric Vehicles
- Neighborhood Electric Vehicles
- Small Task Oriented Vehicles
- Technology evaluation module
- Military power systems
- Stationary energy storage systems

Boston-Power technology advantage:

Compact Footprint	• High energy density results in significant space and weight savings as well as allows electric vehicles to travel more miles per single charge • Modular architecture provides design flexibility to scale from 0.155kWh to several MWh
High Energy Density	• Highest energy density in its class at 171Wh/kg and 329Wh/L • Enables dependable, long runtime across multiple market segments
Long Cycle Life	• Swing Key block supports deep cycling with calendar life up to 10 years • Cell technology promotes wide range of operating temperatures
Safety	• Independent and distributed safety features • Optional monitoring electronics optimize performance and provide redundant safety
Environmental Sustainability	• Batteries developed from sustainable, non-toxic and recyclable materials

Appendix B
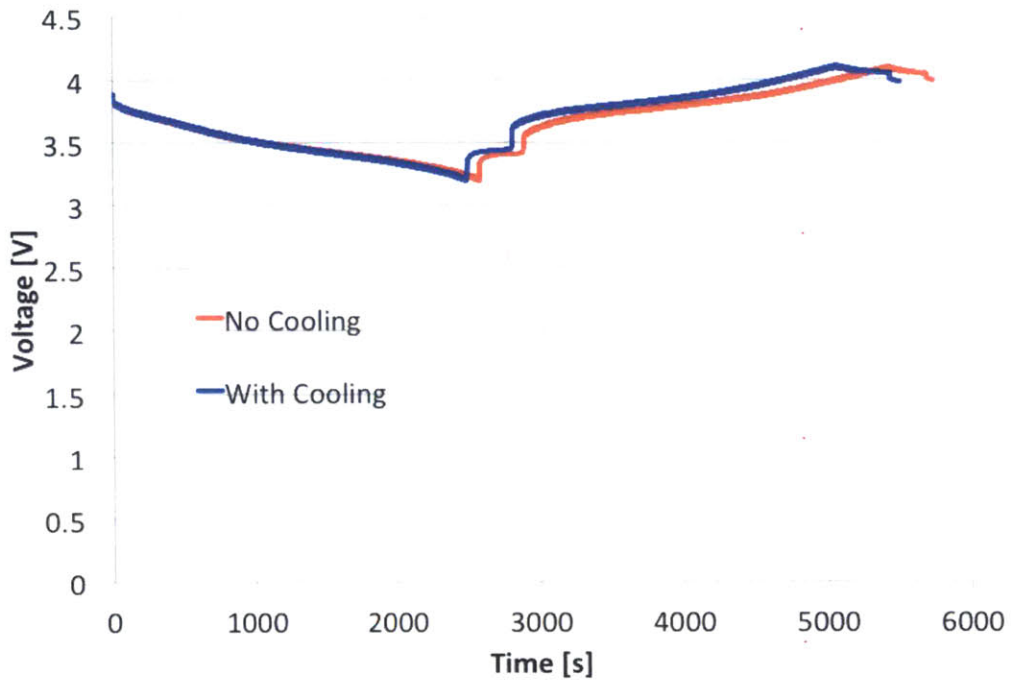## Voltage and Current Data Plotted Versus Time for All Eight Experiments

Figure 29: Voltage data for the one block experiments plotted against experiment time
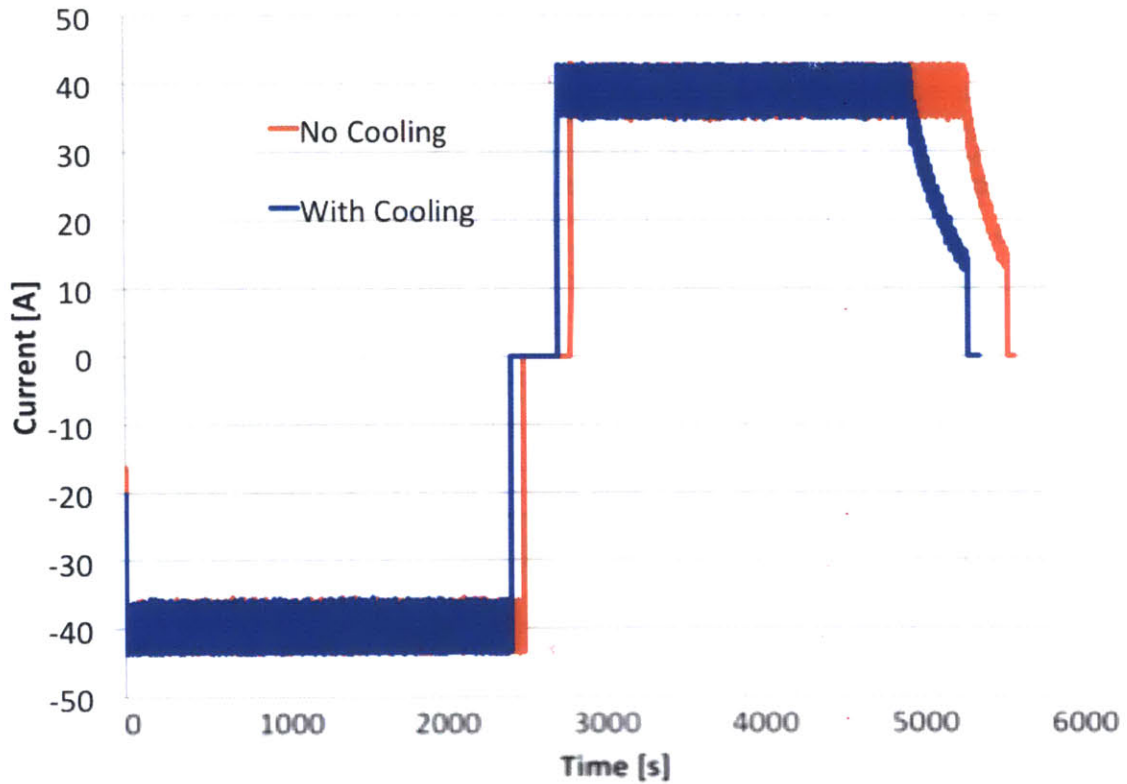

Figure 30: Current data for the one block experiments plotted against experiment time
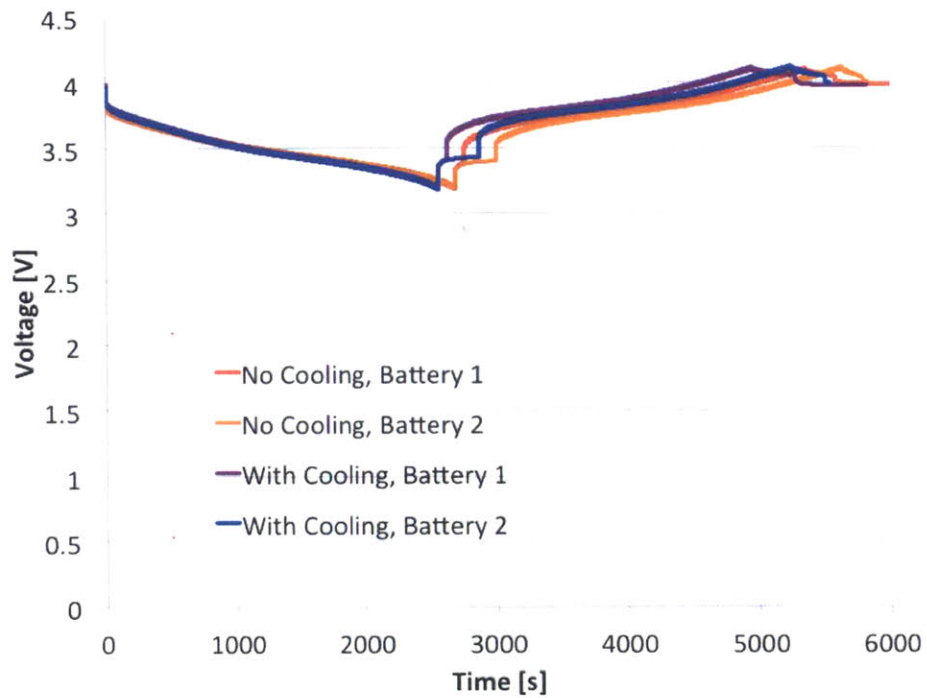
Figure 31: Voltage data for the two block experiments plotted against experiment time
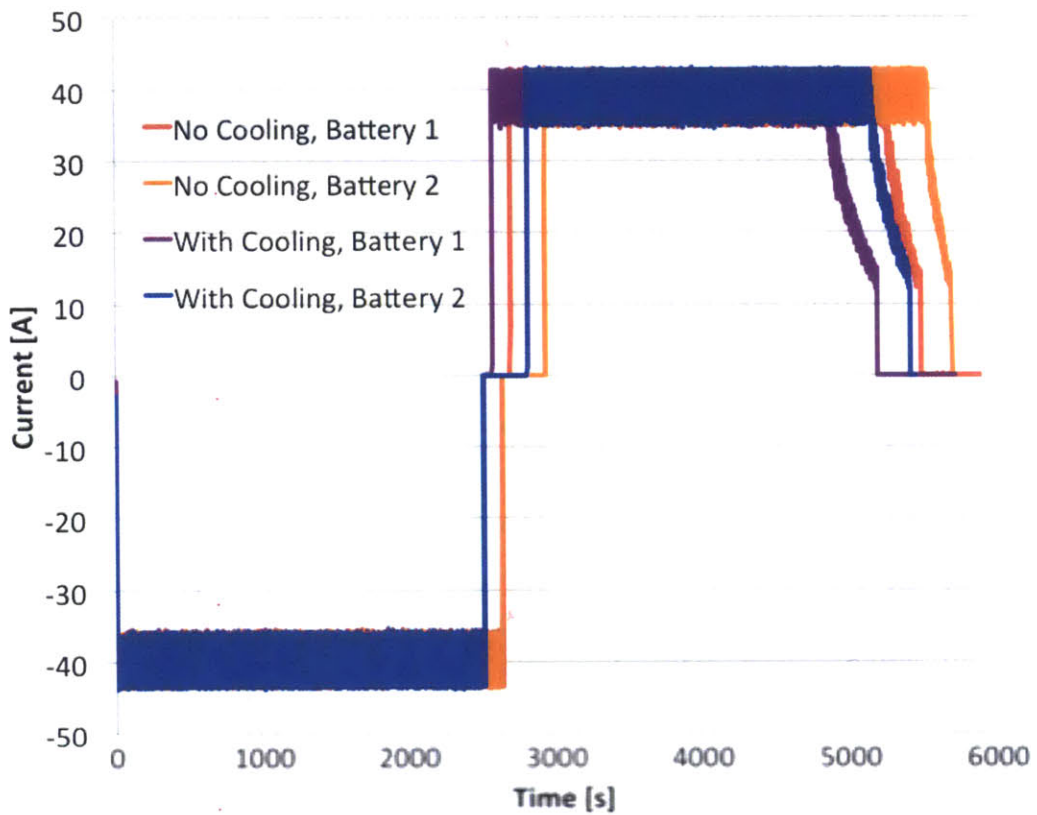

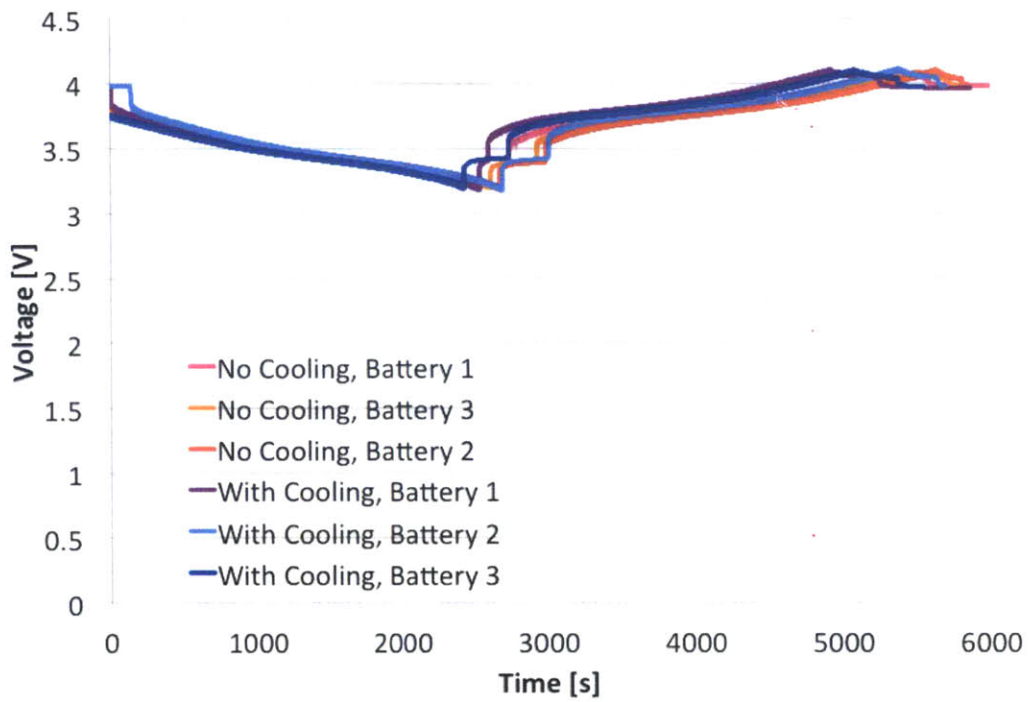Figure 32: Current data for the two block experiments plotted against experiment time

Figure 33: Voltage data for the three block experiments plotted against experiment time
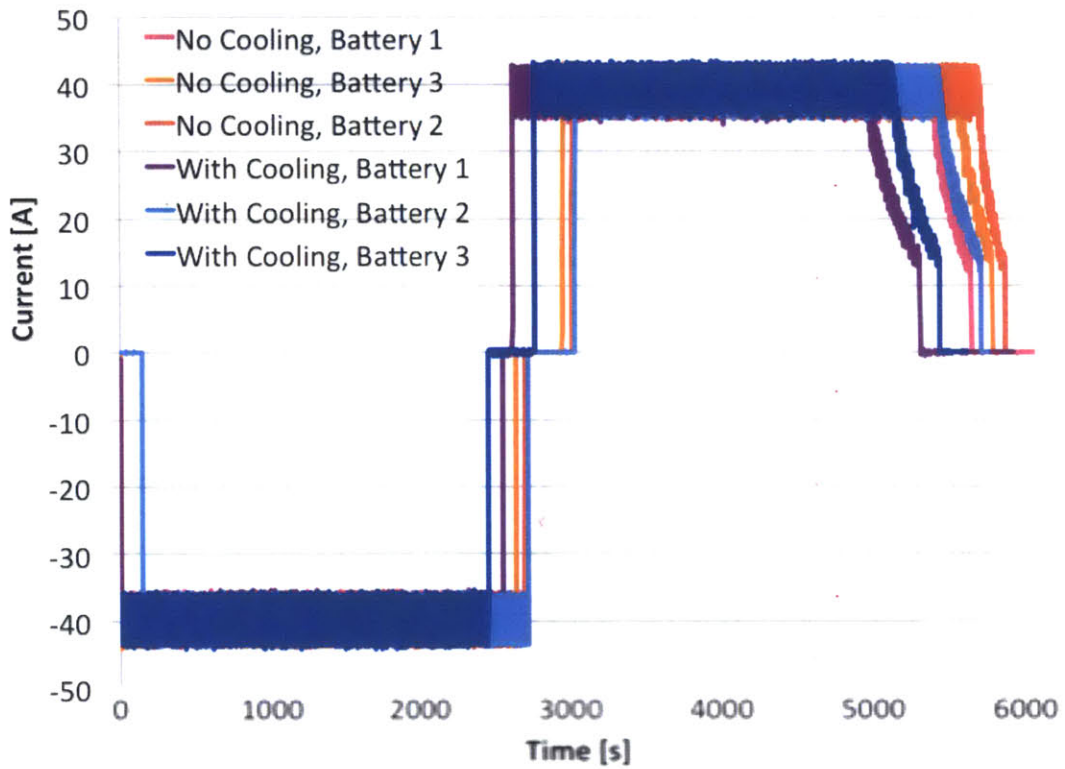

Figure 33: Current data for the three block experiments plotted against experiment time
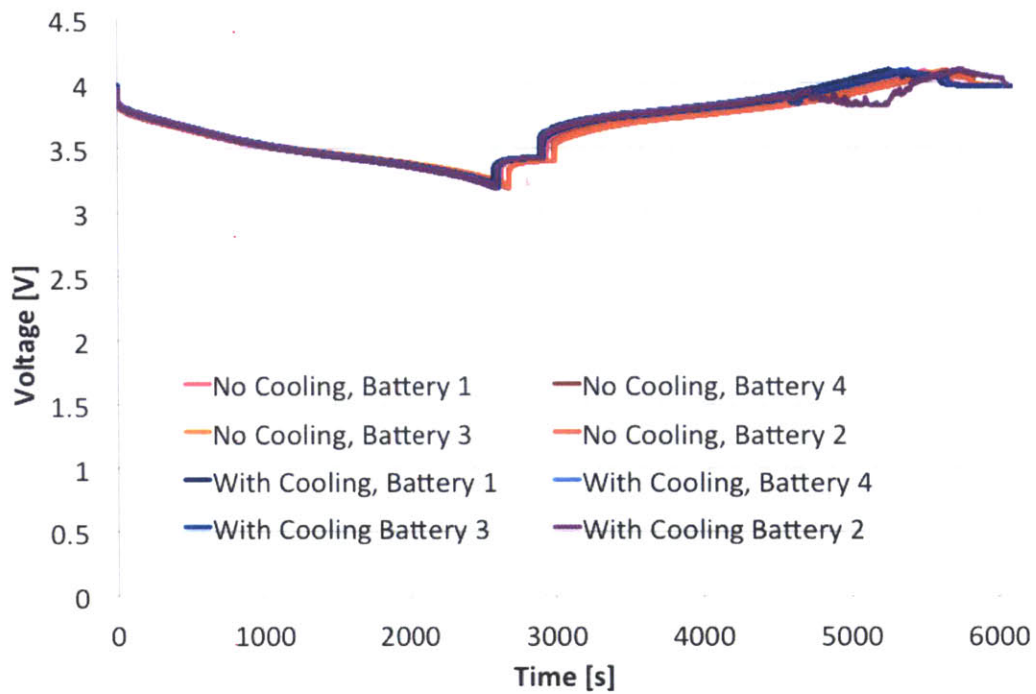
Figure 34: Voltage data for the four block experiments plotted against experiment time
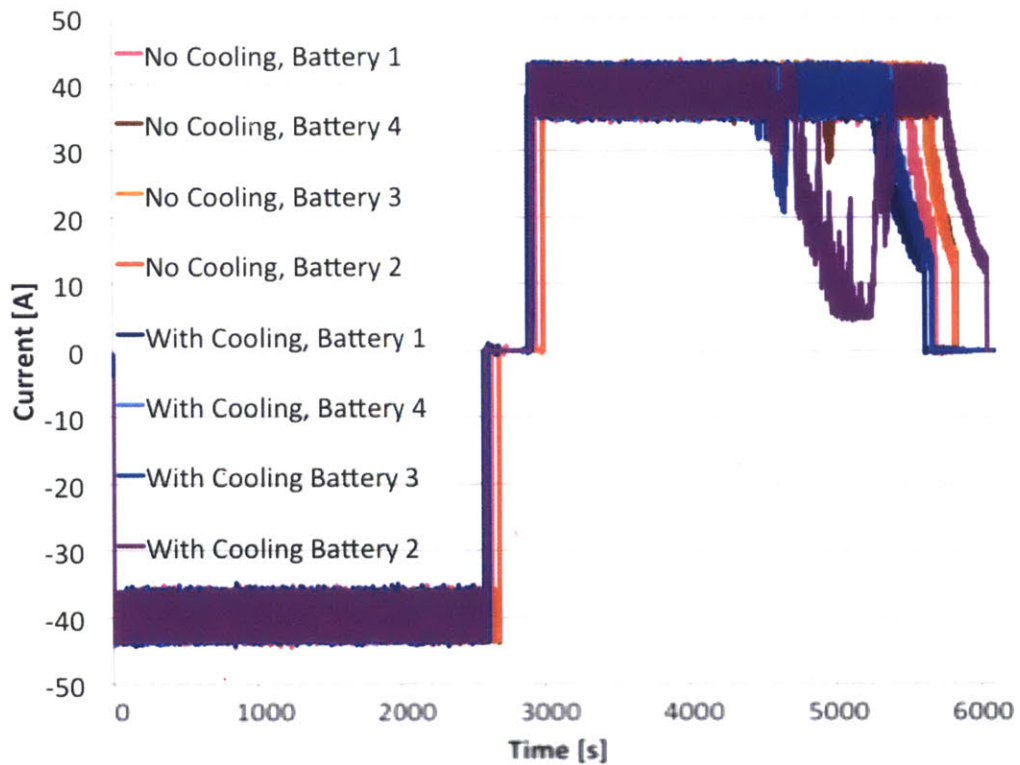

Figure 35: Current data for the four block experiments plotted against experiment time